ACADÉMIE DES SCIENCES
INSTITUT DE FRANCE

Comptes Rendus. Géoscience — Sciences de la Planète
Supplementary material to the article available at:
https://doi.org/10.5802/crgeos.252

Research article

Accretion versus erosion and sediment transfer balance near the subduction interface

Serge Lallemand [*, a], **Michel Peyret** [a], **Diane Arcay** [a] and **Arnauld Heuret** [b]

[a] Geosciences Montpellier, CNRS, Université de Montpellier, Université des Antilles, France

[b] Geosciences Montpellier, CNRS, Université de Montpellier, Université des Antilles, Université de Guyane, France

E-mail: serge.lallemand@umontpellier.fr (S. Lallemand)

Manuscript received 5 July 2023, revised 20 November 2023, accepted 21 December 2023.

1. Sediment thickness, trench depth and margin type database

* Corresponding author.

Supplementary Table S1. Table of measured or estimated parameters (∗) for each profile and transect in the submap database (see submap.fr) with source references

Region	Trench	Lon	Lat	Z_t	T_{SP}	T_{SP}^*	T_{sed}	T_{sed}^*	$T_{channel}$	$T_{channel}^*$	MT	MT*	Sources
	E-Calabria	17.4	40	1.5		7		7	C			1	Heuret [2005], this study
	Calabria	17.7	39.4	2.2		7		7	C			1	Maesano et al. [2017]
		18.8	38	3.4		7		7		2.5		1	Heuret [2005]
		19.2	37.6	3.3	7		7		2.5		1		Cernobori et al. [1996]
		18	36.1	4		6	4.3		3.1			1	Polonia et al. [2017]
		17	35.8	3.9	5.3		7.5		4.8			1	Chamot-Rooke et al. [2005]
		16.6	35.7	3.2	5		5.5		3		1		Maesano et al. [2017]
	W-Calabria	16	36.2	4		5.2		6	3.5			1	Polonia et al. [2017]
	W-Aegean	18.8	37	3.5		5.2		6.5		5		1	Heuret [2005], this study
	Aegean	18.9	35	3.9		5.2		6.5		5		1	Heuret [2005], this study
		19.3	34.2	3.7	5.5		7		5			1	Chamot-Rooke et al. [2005], Chaumillon and Mascle [1997]
MEDITERRANEAN–MIDDLE EAST		19.7	34.1	3.8		5.2		8		5		1	Von Huene et al. [1997b]
		19.8	34	3.7		5.2	9.5			5		1	Lallemant et al. [1994]
		20	33.7	3.7		5.2		10.5		5		1	Heuret [2005], this study
		22	33.2	2.5		5.2		11.5		5		1	Heuret [2005], this study
		22.5	33.3	2.4	5		12.5		5			1	Chamot-Rooke et al. [2005]
		24	33	2.7		5.5		12.5		5		1	Heuret [2005], this study
		26	32.2	3.2		6		12.5		4.5		1	Heuret [2005], this study
		28	33	3.1		6.5	12.5		4			1	Chamot-Rooke et al. [2005]
		28.2	33.1	3.1		7	10			4		1	Chaumillon and Mascle [1997], Huguen et al. [2001], this study
	E-Aegean	30	34.4	2.7		7.5		9.5		?		1	Heuret [2005], this study
	W-Cyprean	31.5	34.6	2.4		8		9		?		1	Heuret [2005], this study
	Cyprean	33.5	34.1	2.3		9		8		?		1	Heuret [2005], this study
	E-Cyprean	33.8	34.3	2	10		7.2		C			1	Vidal et al. [2000]

(continued on next page)

Supplementary Table S1. (continued)

Region	Trench	Lon	Lat	Z_t	T_{SP}	T_{SP}^*	T_{sed}	T_{sed}^*	$T_{channel}$	$T_{channel}^*$	MT	MT*	Sources
	W-Makran	57.5	24.7	1.6		4		7.3		?		1	Heuret [2005], this study
	Makran	59.5	24.2	2.9		4	3		4.7			1	Pajang et al. [2022]
		60.9	24.2	2.9			7		4.7			1	Pajang et al. [2022]
		61.5	24	3.4		4		7.4		4		1	Heuret [2005], this study
		62.8	24.2	3.2	4		7.5		3			1	Kopp et al. [2000], Parvaiz et al. [2022]
		63.5	24.1	3.2		4		7.5	3.6			1	Heuret [2005], this study
	E-Makran	65.5	24.5	2.5		4		7.5		3		1	Heuret [2005], this study
	S-Japan	142.2	35	8.1	0.2			0.5	1.2		2		Tsuru et al. [2002]
	Japan	142.8	36	7.5	0.2		0.5		2		2		Tsuru et al. [2002]
		143.5	37	7.6	0.3			0.4	1.5		2		Tsuru et al. [2002]
		144	38	7.5	0.3		0.4		1.4		2		Kodaira et al. [2012]
		144.2	39	7.3		0.3		0.4	2		2		Tsuru et al. [2000]
		144.3	39.5	6.7	0.3		0.3		1		2		Tsuru et al. [2002], Von Huene et al. [1994]
	N-Japan	144.5	40.5	7.4	0.3			0.4	1		2		Tsuru et al. [2002]
	S-Kurils	145	41.2	7.1	0.3		1			0.7	2		Lallemand et al. [1986], this study
	Kurils	145.5	41.5	7.1		0.3		0.8		0.6		2	Heuret [2005], this study
		146.2	41.8	7.2	0.3		0.7		0.4		2		Schnürle et al. [1995]
NORTH PACIFIC		147	42.2	6.8		0.3		0.4		0.4		2	Heuret [2005], this study
		148.5	43	8.6	0.3		0.4		0.5		2		Klaeschen et al. [1994], Gnibidenko et al. [1983]
		149	43.5	8.7		0.3		0.4		0.5		2	Heuret [2005], this study
		149.2	43.7	9.2	0.3		0.5			0.5		2	Gnibidenko et al. [1983], this study
		149.6	43.9	9.2	0.3		0.5			0.5		2	Gnibidenko et al. [1983], this study
		151	44.4	9	0.3		0.4			?		2	Gnibidenko et al. [1983]
		153.2	45.7	8.2	0.3		0.4			?		2	Gnibidenko et al. [1983]
		153.5	45.7	8.6	0.3		0.2			?		2	Klaeschen et al. [1994]
		153	45.3	8.9		0.3		0.4		?		2	Heuret [2005], this study
		154	46.2	8.2	0.3		0.4			?		2	Gnibidenko et al. [1983]
		155	46.9	7.7	0.3		0.3			?		2	Gnibidenko et al. [1983]
		155.1	47	7.7		0.3		0.4		0.5		1	Heuret [2005], this study
		156	47.8	8.2	0.3		0.5			0.5		1	Gnibidenko et al. [1983], this study

(continued on next page)

Supplementary Table S1. (continued)

Region	Trench	Lon	Lat	Z_t	T_{SP}	T_{SP}^*	T_{sed}	T_{sed}^*	$T_{channel}$	$T_{channel}^*$	MT	MT*	Sources
		157	48.7	8.4	0.3		0.5			0.5		1	Gnibidenko et al. [1983], this study
		157.5	49	7.4		0.3		0.5	0.5			1	Klaeschen et al. [1994]
		158.1	49.2	7.5	0.3		0.5		0.5		1		Klaeschen et al. [1994]
	N-Kurils	158.2	49.4	7.7	0.3		0.6			0.5		1	Gnibidenko et al. [1983], this study
	S-Kamtchatka	159.2	50.2	7.6	0.3		0.4			0.5		1	Gnibidenko et al. [1983], this study
	Kamchatka	160	50.9	7.6	0.3		0.5			0.5		1	Gnibidenko et al. [1983], this study
		160.2	51	6.8		0.3		0.6		0.5		1	Scholl et al. [2015], this study
		160.8	51.6	7.8	0.3		0.8			?		1	Gnibidenko et al. [1983]
		161.2	51.9	7.7	0.3		0.5			?		1	Gnibidenko et al. [1983]
		161.8	52.4	7.6	0.4		0.5			?		1	Gnibidenko et al. [1983]
		162	52.7	7.6	0.6		0.6			?		1	Gnibidenko et al. [1983]
		162.3	53	7.6	0.7		0.6			?		1	Gnibidenko et al. [1983], Baranov et al. [2022]
		162.8	53.3	7.4	1		1			?		1	Baranov et al. [2022]
		163	53.7	6.4	0.8		0.5			?		1	Gnibidenko et al. [1983], Baranov et al. [2022]
		163.2	54	6.4	1		0.5			?		1	Gnibidenko et al. [1983]
		163.4	54.3	5.9	2		2			?		1	Baranov et al. [2022]
		164	54.7	6.2		1	0.5			?		1	Gnibidenko et al. [1983]
	N-Kamtchatka	164	55.5	5.4		1		0.5		?		1	Gnibidenko et al. [1983]
	W-Aleutians	164	55.3	5.6		1	1			?		?	Gnibidenko et al. [1983]
	Aleutians	165	54.9	6		1		1		?		?	Heuret [2005], this study
		165.3	54.5	6.9		1	1			?		?	Gnibidenko et al. [1983]
		166	54	6.9		1	2			?		?	Gnibidenko et al. [1983]
		167	53.8	6.5		0.5		2		?		?	Heuret [2005], this study
		169	52.9	6.4		0.3		2		?		?	Heuret [2005], this study
		171	52.1	6.4		0.3		2		?		?	Heuret [2005], this study
		173	51.6	7.0		0.3		2		?		?	Heuret [2005], this study
		175	51.1	7.3		0.3		2		?		?	Heuret [2005], this study
		177	50.8	7.3		0.3		1.5		?		?	Scholl et al. [2015]
		179	50.4	7.3		0.3		1.5		?	2		Scholl et al. [2015]
		181	50.3	7.2		0.3		2		?	2		Jicha and Kay [2018]
		183	50.4	7.4		0.3		2		1.2	2		Scholl et al. [2015], Jicha and Kay [2018], this study
		183.9	50.5	7.1	0.3		1		1.2			2	McCarthy and Scholl [1985]

(continued on next page)

Supplementary Table S1. (continued)

Region	Trench	Lon	Lat	Z_t	T_{SP}	T_{SP}^*	T_{sed}	T_{sed}^*	$T_{channel}$	$T_{channel}^*$	MT	MT*	Sources
		184	50.5	7.2		0.3	2		1.2		2		Ryan and Scholl [1989], Jicha and Kay [2018]
		184.9	50.6	7	0.2		1.1		1.5			2	McCarthy and Scholl [1985]
		185	50.5	7.2	0.3		1.2		1.1			2	Scholl et al. [1982], Von Huene and Miller [1986]
		186	50.8	7.2		0.3	1.1		1.1			2	Ryan and Scholl [1989]
		186.6	50.8	7.3		0.2	2.3		1.3			2	Ryan and Scholl [1989], Scholl et al. [1982], McCarthy and Scholl [1985]
		186.8	50.7	7.2		0.3	1.1			1.3		2	Scholl et al. [1982], this study
		187	50.8	7.3		0.3	3			1.5		2	Scholl et al. [1982], this study, McCarthy and Scholl [1985]
		187.2	50.9	7.3		0.4	3.8		1.9			2	Ryan and Scholl [1989]
		187.4	50.8	7.2		0.4	4			1.9		2	Scholl et al. [1982], this study
		189	51.1	7.3		0.4		2		1.9		NA	Heuret [2005], this study
		191	51.5	7.2		0.4		2		?		NA	Heuret [2005], this study
		193	52	7.2		0.4		2		?		NA	Heuret [2005], this study
	E-Aleutians	195	52.5	6.9		0.4		1		?		NA	Heuret [2005], this study
	W-Alaska	197	53.1	6.5	0.4		0.9			?		NA	Scholl et al. [1982]
	Alaska	198.2	53.3	6.7		0.4	1.3			?		1	Lewis et al. [1988]
		199	53.5	6.9		0.4		1.2		1		1	Heuret [2005], this study
		199.5	53.5	6.6		0.4	1.1			1		1	Lewis et al. [1988], this study
		199.9	53.5	5.5		0.4	2		1			1	Lewis et al. [1988]
		201	53.8	6.4		0.4		1.5		0.9		1	Scholl et al. [2015], this study
		203	54.1	5.8	0.4		1		0.8			1	von Huene et al. [2021], Lewis et al. [1988], Von Huene and Miller [1986]
		203.5	54.2	5.8		0.4	1.4		1			1	von Huene et al. [2021], Lewis et al. [1988]
		205	54.8	5.6		?		1.7		1		1	Heuret [2005], this study
		207	55.6	5.4		?		2		1.7		1	Scholl et al. [2015], this study
		208	56	5.5		?	2.8		1.7			1	Von Huene and Miller [1986]
		209	56.2	5.4		?		2.7		1.7		1	Heuret [2005], this study
		209.8	56.6	5.3		?	2.7			1.6		1	Von Huene [1972], this study
		211	57.1	5.1		?		2.6		1.5		1	Heuret [2005], this study
		211.2	57.1	4.9		?	2.5			1.5		1	Von Huene [1972], this study
		211.3	57.2	4.8	1.5		2.4			1.4		1	Von Huene [1972], this study

(continued on next page)

Supplementary Table S1. (continued)

Region	Trench	Lon	Lat	Z_t	T_{SP}	T_{SP}^*	T_{sed}	T_{sed}^*	$T_{channel}$	$T_{channel}^*$	MT	MT*	Sources
		212	57.4		1.2		2.7			1.3		1	Von Huene [1972], this study
		212.1	57.4	4.9	0.8		2.5		1.2		1		Fruehn et al. [1999], Von Huene and Klaeschen [1999]
		212.9	57.9	4.8	1		2.3		1.6		1		Fruehn et al. [1999]
		213	58	4.9		1		2.5		1.6		1	Heuret [2005], this study
		213.2	58.2	4.9	1		2.6		1.6		1		Fruehn et al. [1999]
		213.6	58.6	4.5	0.9		4		1.3		1		Fruehn et al. [1999]
		214.3	59.1	4.5		?	2		2			1	Fruehn et al. [1999]
		214.5	59.1	4.5		?		2		2		1	Scholl et al. [2015], this study
		215	59.1	4.2		?		2		?		1	Scholl et al. [2015]
	E-Alaska	215.5	59.2	3.3		?	2.7		0			1	Brocher et al. [1994]
	N-Cascadia	231.7	50	2.1		?		2.8		?		1	Heuret [2005], this study
	Cascadia	233	48.4	2.6		?	2.9			?		1	Davis et al. [1990], Yuan et al. [1994]
		233.4	48	2.7		2		3		0.5		1	Heuret [2005], this study
		233.5	48.1	2.4		2	3			0.6		1	Davis et al. [1990], this study
		233.9	47.3	2.4		2	3		0.7			1	Han et al. [2017]
		234	47	2.7		2		3	0.6			1	Han et al. [2017], this study
		234.1	46.8	2.4	2			3.5	0.3			1	Han et al. [2017], this study
		234.4	46	2.5		2		3.5	0			1	Han et al. [2017]
		234.6	45.1	2.6		2	4		0.5			1	Tobin et al. [1993], Han et al. [2017]
		234.6	44.7	2.9		?	3.5		1.8			1	Wang et al. [1994, 1990], Von Huene and Miller [1986], Han et al. [2017]
		234.6	44	3.0		?		3.5				1	Heuret [2005], this study
	S-Cascadia	234.7	42	3.1		?		3.5				1	Heuret [2005], this study
CENTRAL & SOUTH AMERICA–CARIBBEANS–SCOTIA	W-Central_America	253.7	20.3	3.8		0.5	1.6			?	1		Bartolomé et al. [2011], this study
	Central_America	253.7	20	4.3	0.5		0.7			?	1		Bartolomé et al. [2011], Prada et al. [2023]
		254.5	19.1	5.0		0.4		0.7		?	2		Scholl et al. [2015], Prada et al. [2023]
		254.9	18.8	5.0	0.2		0.2		0.4		2		Prada et al. [2023]
		256	17.9	4.9		0.2		0.2		?	2		This study, Prada et al. [2023]
		258	16.9	4.6		0.2		0.2		?		2	This study
		260	16.3	5.2		0.2		0.3		?		2	This study
		261	15.9	5.1	0.2		0.4		0.3			2	Shipley and Moore [1985], Von Huene and Miller [1986], Moore and Shipley [1988]

(continued on next page)

Supplementary Table S1. (continued)

Region	Trench	Lon	Lat	Z_t	T_{SP}	T_{SP}^*	T_{sed}	T_{sed}^*	$T_{channel}$	$T_{channel}^*$	MT	MT*	Sources
		261.6	15.7	5.2		0.3	0.4			?		2	Shipley and Moore [1985]
		262	15.6	5.1		0.3		0.7		?		2	Scholl et al. [2015]
		264	15.3	5.5		0.3		0.7		?		2	Scholl et al. [2015]
		266	14.2	6.5		0.3		0.7		?		2	Scholl et al. [2015]
		268	13.2	6.3		0.4		0.7		?		2	Scholl et al. [2015]
		269	12.7	6.1		0.4	0.6			?		2	Shipley and Moore [1985], Moore et al. [1986]
		269.2	12.6	5.9	0.4		0.5			?	2		Ranero and von Huene [2000], Ladd et al. [1982]
		270	12.3	5.8		0.4		0.6		?		2	Heuret [2005], this study
		272	11.4	5.3		0.4		0.6		0.7		2	Heuret [2005], this study
		272.4	11.3	5.4	0.4		0.7		0.7		2		Ranero and von Huene [2000], Ranero et al. [2007]
		273.3	10.3	5.1		0.4	0.8			0.6	2		Ranero et al. [2003], this study
		273.2	10.2	5		0.4	0.6			0.6	2		Ranero et al. [2008, 2003], this study
		273.5	10	4.9		0.4	0.7			0.6	2		Ranero et al. [2003], this study
		273.8	9.6	4.4	0.4		0.6		1		2		Shipley et al. [1992], Tobin et al. [2001], Shipley and Moore [1986], Ranero et al. [2007], Shipley and Moore [1985], Von Huene and Miller [1986], Shipley et al. [1990]
		274	9.4	3.8		0.4	0.7		0.9		2		Hinz et al. [1996]
		274.3	9.2	3.6		0.4	0.5		0.4		2		von Huene et al. [2004]
		274.5	9.1	3.6		0.4	0.4		0.5		2		Hinz et al. [1996], von Huene et al. [2004, 2000]
		274.8	9	3.7		0.5	0.6		0.7		2		Hinz et al. [1996], von Huene et al. [2000]
		275.4	8.3	3		0.5	0.2			0.6	2		Ranero et al. [2008], this study
		275.6	8.6	2.8		0.5	0.4		0.5		2		Hinz et al. [1996]
		275.7	8.5	2.6		0.6	0.5		1		2		Ranero et al. [2008], von Huene et al. [2000]
		276	8.4	3.0		0.7		1.4		1		2	Heuret [2005], this study
		278.9	6.8	3	0.8		0.9		0.4		1		MacKay and Moore [1990], Silver et al. [1990]
		279.1	6.7	3.5	0.6		1.3		0.3		1		MacKay and Moore [1990]
	E-Central_America	279.3	6.7	3.5		0.6	1.6		0.6		1		MacKay and Moore [1990]
	W-Panama	279	10	3.0		0.6		2		?		1	Heuret [2005], this study
	Panama	279.7	10.3	3.5	0.6		2.5			?	1		Silver et al. [1990]
		280.5	10.5	3.6		0.6		2		?		1	Heuret [2005], this study
		280.7	10.6	3.5		0.6	2			?	1		Silver et al. [1990]
		282	10.4	3.3		0.6		2		?		1	Heuret [2005], this study
	E-Panama	282.3	10.2	3.3		0.6	1.6			?	1		Silver et al. [1990]

(continued on next page)

Supplementary Table S1. (continued)

Region	Trench	Lon	Lat	Z_t	T_{SP}	T_{SP}^*	T_{sed}	T_{sed}^*	$T_{channel}$	$T_{channel}^*$	MT	MT*	Sources
	W-Venezuela	283.5	10	3	2		4		0		1		Mantilla-Pimiento et al. [2009], Sanchez et al. [2019]
	Venezuela	285	12.2	3.7		2.5		4		?		1	Heuret [2005], this study
		285.3	12.1	3.7	3		3.6			?		1	Sanchez et al. [2019]
		285.7	12.1	3.7		3	4			?		1	Kroehler et al. [2011]
		286	12.7	3.7		3	4			?		1	Kroehler et al. [2011]
		287	13.4	4.1		2.5		1.8		?		1	Heuret [2005], this study
		289	13.8	4.6		2		1.8		?		1	Heuret [2005], this study
		290.2	13.6	4.9	1.4		1.8			?		1	Kroehler et al. [2011], Ladd et al. [1984]
		291	13.5	5.1		1.7		1.8		?		1	Heuret [2005], this study
		292.2	13.3	5	2		3.6		1.4			1	Kroehler et al. [2011], Ladd et al. [1984]
		293	13.1	5.1		3		3.8		1.3		1	Heuret [2005], this study
	E-Venezuela	294.6	12.3	4.7	4		4		1			1	Kroehler et al. [2011]
	W-Muertos	290	17.3	5.0		1.4	0.3		0.1			1	Granja-Bruña et al. [2014]
	Muertos	291	17.2	5.6		1.4	0.8		0.4			1	Granja-Bruña et al. [2014]
		292	17.2	5.4	1.4		1.5		0.7			1	Granja-Bruña et al. [2009], Sanchez et al. [2019]
	E-Muertos	294	17.2	5.0		1.4	1.3		0.7			1	Granja-Bruña et al. [2009]
	W-Hispaniola	287.6	20.3	4.2	1		2.3		C			2	Rodríguez-Zurrunero et al. [2020a,b]
	Hispaniola	288	20.4	4.3	1.4		3		C			2	Rodríguez-Zurrunero et al. [2020a,b]
		289.3	20.2	4.1	0.4		2.3		C			2	Rodríguez-Zurrunero et al. [2020a,b]
		290	20	3.9		0.4		2.5	C			2	Heuret [2005], this study
	E-Hispaniola	290.7	19.7	4	0.4		2.5		C			2	Rodríguez-Zurrunero et al. [2020a,b]
	W-Puerto-Rico	292	19.6	8.3		0.4	1		C			2	Rodríguez-Zurrunero et al. [2020a,b]
	Puerto-Rico	293.5	19.7	8.2		0.4	2.5		C			2	Ten Brink [2005]
		294	19.8	8.2		0.4		2	C			2	Ten Brink [2005]
	E-Puerto-Rico	295	19.7	8		0.3		2	C			2	Ten Brink [2005]
	N-Lesser_Antilles	296	19.8	7.6		0.3	0.2			0.2		2	Ten Brink [2005], this study
	Lesser_Antilles	297	19.7	7.7	0.3		0.5		0.2			2	Morena et al. [2022], Laurencin [2017], Marcaillou et al. [2021], this study
		297.4	19.6	6.3	0.3		0.5		0.2			2	Marcaillou et al. [2021], this study
		298	19.3	6.3	0.3		0.1		0.3			2	Morena et al. [2022], Laurencin [2017], Marcaillou et al. [2021], this study
		299	18.9	6.5	0.4		0.7		0.3		2		Morena et al. [2022], Laurencin [2017], Boucard et al. [2021], Marcaillou et al. [2021], this study

(continued on next page)

Supplementary Table S1. (continued)

Region	Trench	Lon	Lat	Z_t	T_{SP}	$T_{SP}{}^*$	T_{sed}	$T_{sed}{}^*$	$T_{channel}$	$T_{channel}{}^*$	MT	MT*	Sources
		299.2	18.7	7	0.6		0.7		0.4		2		Marcaillou et al. [2021], this study
		299.3	18.6	6.3	0.7		0.7		0.4		2		Marcaillou et al. [2021], this study
		299.5	18.4	6.1	0.7		0.7		0.5		2		Marcaillou et al. [2021], this study
		299.8	18	6.2	0.6		0.8		0.3			2	Morena et al. [2022], Laurencin [2017], Marcaillou et al. [2021], this study
		300.2	17.6	6.3	0.3		0.7		0			2	Laigle et al. [2013], this study
		300.8	17	6	0.2		0.2		0			2	Morena et al. [2022], Laigle et al. [2013], this study
		301.2	16	5.2	2		1		0.6		2		Westbrook et al. [1988], Boucard et al. [2021], Pichot et al. [2012], this study
		301.4	15.5	5.7	2		0.9		0.5			1	Deville and Mascle [2012], Pichot et al. [2012], this study
		302	15	4		2		5.5		?		1	Morena et al. [2022], this study
		302.3	14	5.7		2		5.5		2		1	Heuret [2005], this study
		302.4	13	4.6	3		5.4		2.1		1		Morena et al. [2022], Speed and Larue [1982], this study
		302.6	12	4	6.3		6.3		1.7		1		Gomez [2018], this study
	S-Lesser_Antilles	302.4	11	3.8	5		6		2		1		Morena et al. [2022], Deville and Mascle [2012], Gomez [2018], this study
	N-Colombia	281.3	7	4	0.6		0.6		0.3		1		Westbrook et al. [1995]
	Colombia	281.5	6.8	4.1	0.6		1		0.3		1		Westbrook et al. [1995]
		281.9	5	3.8		0.6		1		0.5		1	Heuret [2005], this study
		280.9	3.5	3.9		0.6	1.8		0.6			2	Marcaillou et al. [2006]
		280.9	3.2	3.9		0.6	2			0.7		2	Marcaillou et al. [2006], this study
		280.6	2.9	3.9		0.7	3.7			0.8		2	Marcaillou et al. [2006], this study
		280.5	2.7	3.6		0.7	4.4			1.9		2	Marcaillou et al. [2006], this study
		280.3	2.5	3.6		0.7	3.9			2.1		2	Marcaillou et al. [2006], this study
		280.5	2.3	3.6	0.7		4.4		2.3		2		Collot et al. [2004], Marcaillou et al. [2006]
		279.9	2	3	0.1		3.5		1		2		Collot et al. [2004], Marcaillou et al. [2006]
		280.1	1.8	3.1		0.2	2.8		1.1		2		Collot et al. [2008, 2004], Marcaillou et al. [2006], Agudelo et al. [2009]
	S-Colombia	279.9	1.7	3.4		0.3	2.8		2.2		2		Marcaillou et al. [2006]

(continued on next page)

Supplementary Table S1. (continued)

Region	Trench	Lon	Lat	Z_t	T_{SP}	T_{SP}^*	T_{sed}	T_{sed}^*	$T_{channel}$	$T_{channel}^*$	MT	MT*	Sources
	N-Ecuador	279.3	0.4	3.6		0.4	1		0.3		2		Marcaillou et al. [2016]
	Ecuador	279.2	0.3	3.7		0.5	1		0.8		2		Marcaillou et al. [2016]
		279	0	3.3		0.5		0.3		0.6		2	Heuret [2005], this study
		278.9	−0.4	3	0.5		0.3			0.4		2	Collot et al. [2004]
		278.5	−1.4	3.5		0.5	0.8		0		2		Collot et al. [2017]
		278.5	−1.6	3.4		0.5	0.2		0.3		2		Sage et al. [2006]
		278.5	−1.7	3.4		0.5	0.4		0.6		2		Sage et al. [2006]
	S-Ecuador	278.5	−2	3.7		0.5		0.3		0.7		2	Heuret [2005], this study
	N-Peru	278.3	−3.3	4.8		0.5	1		1		2		Collot et al. [2011]
	Peru	278.1	−4	4.8		0.4		1		0.9		2	Heuret [2005], this study
		278.1	−5.5	5.3	0.3		1.3		0.7		2		von Huene et al. [1989], Von Huene and Miller [1986]
		278	−5.6	5.1	0.5		1.4		1		2		von Huene et al. [1996]
		278.4	−7	5.8		0.3		1		0.7		2	Heuret [2005], this study
		279.2	−9	6.3		0.3		1		0.7		2	Heuret [2005], this study, von Huene et al. [1996]
		279.2	−9.2	6.5	0.3		0.9		0.7		2		Von Huene et al. [1985], Von Huene and Miller [1986], von Huene et al. [1996]
		279.2	−9.3	6.2		0.3	1.1		0.9			2	von Huene et al. [1996]
		280.4	−11	6.3		0.3		0.4		0.8		2	Heuret [2005], this study
		281	−12	6.1		0.3	0.4		0.8		2		Pecher et al. [2001]
		281.7	−13	5.9		0.2		0.4		0.8		2	Heuret [2005], this study
		283.4	−15	4.7		0.2		0.4		?		2	Heuret [2005], this study
		283.6	−15.2	4.9		0.2	0.5			?	2		Hampel et al. [2004]
	S-Peru	285.9	−17	6.9		0.1		0.4		?		2	Heuret [2005], this study
	N-Chile	288	−19	7.0		0.1		0.4		1.5		2	Heuret [2005], this study
	Chile	288.5	−19.5	7.3	0.1		0.1		1.5		2		Ma et al. [2022], Myers et al. [2022], González et al. [2023]
		288.7	−20	7.7	0.1		0.1		1		2		Petersen et al. [2021], González et al. [2023], Ma et al. [2023]
		288.8	−20.5		0		0		1		2		Ma et al. [2023]
		288.8	−20.8	7.7	0.1		0.1		1.5		2		Ma et al. [2022]
		288.7	−21	6.9		0.1		0.1		1.5		2	Heuret [2005], this study
		288.7	−23	7.9		0.1		0.1		0.3		2	Heuret [2005], this study

(continued on next page)

Supplementary Table S1. (continued)

Region	Trench	Lon	Lat	Z_t	T_{SP}	T_{SP}^*	T_{sed}	T_{sed}^*	$T_{channel}$	$T_{channel}^*$	MT	MT*	Sources
		288.6	−23.5	7.9	0.1		0.1		0.2		2		Contreras-Reyes et al. [2010], von Huene and Ranero [2003], this study
		288.6	−25	7.5		0.1		0.1		?		2	Heuret [2005], this study
		288.3	−27	7.5		0.1		0.1		?		2	Heuret [2005], this study
		287.7	−29	6.2		0.1	0.2			?		2	Contreras-Reyes and Osses [2010]
		287.5	−30.5	6.1		0.2	0.3			?		2	Contreras-Reyes and Osses [2010]
		287.4	−32	5.8		0.2	0.5			0.9		2	Contreras-Reyes and Osses [2010], this study
		287.4	−32.1	6.1		0.1	0.6			0.9		2	Von Huene et al. [1997a]
		287.3	−32.7	5.8	0.1		1		1			2	Grevemeyer et al. [2003]
		287.2	−33	5.8		0.2	1.8		0.9			2	Contreras-Reyes et al. [2010], this study
		287	−33.4	5.4		0.2	2		1.8			1	Grevemeyer et al. [2003]
		286.9	−34	5.4		0.3	1.2			1		1	Contreras-Reyes and Osses [2010], this study
		286.2	−35.5	5.2		0.3	2		1		1		Contreras-Reyes et al. [2010]
		286.8	−36	5.1		0.3	2.3		1		1		Contreras-Reyes et al. [2010], Grevemeyer et al. [2003]
		286	−36.3	4.9	0.3		2		0.8		1		Contreras-Reyes et al. [2010], Grevemeyer et al. [2003]
		285.6	−36.5	4.3		0.3	2		1		1		Contreras-Reyes et al. [2010], this study
		285.4	−37	4.8		0.3		2.1		0.8		1	Heuret [2005], this study
		285.9	−37.9	4.6	0.3		2		0.5		1		Contreras-Reyes et al. [2010]
		285.4	−37.8	4.6		0.3	2.2		0.5		1		Contreras-Reyes et al. [2010], this study
		285.2	−38.2	4.5		0.4	2.2		0.5		1		Contreras-Reyes et al. [2010], this study
		284.9	−39	4.4		0.4	1.6		1.2		2		Contreras-Reyes et al. [2010]
		285.8	−39.2	4.4		0.5	1.7		0.6		2		Contreras-Reyes et al. [2010], Grevemeyer et al. [2003]
		284.7	−41	3.7		0.6	2.4			1		2	Contreras-Reyes et al. [2010], this study
		284.5	−42.8	3.7		0.7	2.4			1.4		2	Contreras-Reyes et al. [2007], this study
		284.5	−43	4	0.7		2.4		1.5		2		Contreras-Reyes et al. [2010]
		284.1	−44.5	4.2		0.5	2		1.8		2		Contreras-Reyes et al. [2010], Scherwath et al. [2009]
		283.9	−45	3.3		0.4	1.1			1.5		2	Contreras-Reyes and Osses [2010], this study
		284.2	−45.5	3.2		0.3	1.5		1.2		2		Contreras-Reyes et al. [2010]
		284	−45.6	3.3	0.2		1		1.2			2	Scherwath et al. [2009]
	Chile Rise axis	284.4	−46	3.8		0.2	0			1.2	2		Contreras-Reyes and Osses [2010], this study

(continued on next page)

Supplementary Table S1. (continued)

Region	Trench	Lon	Lat	Z_t	T_{SP}	T_{SP}*	T_{sed}	T_{sed}*	$T_{channel}$	$T_{channel}$*	MT	MT*	Sources
	Chile	283.8	−47	3.7		0.2	1.2			1.2		2	Contreras-Reyes and Osses [2010], this study
		283.9	−48	3.9		0.3	1.3			?		2	Contreras-Reyes and Osses [2010]
		282.8	−49	4.0		0.4	1.5			?		2	Contreras-Reyes and Osses [2010]
		283.1	−50	4		0.5	1.5			?		2	Contreras-Reyes and Osses [2010]
		283.3	−51	3.9		0.8		2.8		2.9		2	Heuret [2005], this study
		283.5	−51.3	4	1		2.9		2.9		2		Polonia et al. [2007]
		283.6	−51.8	4		1.1	2.7			2.7		2	Polonia et al. [2007], this study
		283.7	−52.3	4.1	1.2		3.2		2.4		2		Polonia et al. [2007]
		283.9	−53	4.2		1.1	2.5			2.4	2		Polonia et al. [2007], this study
		284.5	−54.1	4.2		1	2.5			2.4		1	Polonia et al. [2007], this study
		285.5	−54.7	4.3	1		3.4		2.5		1		Polonia et al. [2007]
		285.9	−54.9	4.3	1		3.8		1.5		1		Polonia et al. [2007]
		285.7	−55	4.4		1	3.4			1.4		1	Polonia et al. [2007], this study
		287.5	−55.8	4.4	1		2.1		0.5		1		Polonia et al. [2007]
		288	−56	4.4		1	2.3			0.5		1	Polonia et al. [2007], this study
	S-Chile	291.2	−57	4.4		1	2.2			0.5		1	Polonia et al. [2007], this study
	N-Sandwich	329	−54.8	6.4		0.5		0.9		?	2		Heuret [2005], this study
	Sandwich	331	−54.9	7.9		0.5		0.9		?	2		Heuret [2005], this study
		333	−55.1	7.8		0.5		0.9		?	2		Heuret [2005], this study
		334.9	−56	7.3		0.5		0.9		?	2		Heuret [2005], this study
		335.4	−56.7	7.9	0.5		0.9			?	2		Vanneste and Larter [2002]
		335.6	−56.8	7.7	0.4		0.7			?	2		Vanneste and Larter [2002]
		335.9	−57.2	7.5	0.3		0.5			?	2		Larter et al. [2003]
		336.2	−58	7.2		0.3		0.5		?	2		Heuret [2005], this study
		335.7	−59.9	6.6	0.2		0.4			?	2		Larter et al. [2003]
	S-Sandwich	335.4	−60	6.6		0.2		0.5		?	2		Heuret [2005], this study

(continued on next page)

Supplementary Table S1. (continued)

Region	Trench	Lon	Lat	Z_t	T_{SP}	T_{SP}^*	T_{sed}	T_{sed}^*	$T_{channel}$	$T_{channel}^*$	MT	MT*	Sources
	N-Andaman	92.1	14	3.0		1.2	2.2			?		1	McNeill and Henstock [2014]
	Andaman	91.6	12	3.3		1.1		2.4		0		1	Heuret [2005], this study
		91.4	10	3.7	1		2.6		0			1	McNeill and Henstock [2014], Moeremans et al. [2014]
		91.7	8	3.9		0.9		3.4		0		1	Heuret [2005], this study
		92.1	7	4.3		0.8	4.2			?	1		McNeill and Henstock [2014], Moeremans et al. [2014]
	S-Andaman	92.6	6	4.3		0.7		4.1		?		1	Heuret [2005], this study
	N-Sumatra	93	4	4.5		0.6	4.3			?		1	McNeill and Henstock [2014], Moeremans et al. [2014]
		95.2	2.1	4.1		0.5	5.8			?		1	Franke et al. [2008]
	Sumatra	95.7	2	4.1		0.5	3		1.2			1	McNeill and Henstock [2014], Moeremans et al. [2014], Franke et al. [2008]
		96	1.6	4.2		0.5	4.8			?		1	Franke et al. [2008]
		97	0	5.3		0.3		2.5		?		1	Heuret [2005], this study
SOUTHEAST ASIA		97.7	−1	6		0.2	1.8			?	1		McNeill and Henstock [2014], this study
		98.1	−2	5.8	0.1		0.8			?		1	Moeremans et al. [2014]
		99.7	−4	5.5		0.2		1.3		0		1	Heuret [2005], this study
		99.9	−4.9	6		0.2	1.7		0		1		Moeremans et al. [2014]
		100.8	−5.5	6	0.2		0.8		0			1	Moeremans et al. [2014]
	S-Sumatra	102.3	−7	6.2		0.3	1.1			0.2		1	McNeill and Henstock [2014], this study
	W-Java	104.2	−8	6.5	0.5		1.7		0.4			1	Kopp [2011]
	Java	105	−8.4	6.7		0.5		1.5		0.6		2	Heuret [2005], this study
		106.3	−9.4	6.5	0.5		1.6		0.8			2	McNeill and Henstock [2014], Kopp [2011], Kopp et al. [2009]
		107	−9.7	6.7		0.5		1.5		0.8		2	Heuret [2005], this study
		109	−10.5	6.8		0.5		1.2		?		2	Heuret [2005], this study
		109.7	−10	6.5		0.5	1			?		2	Kopp [2011]
		110.4	−10.3	7.5		0.5	1			?		2	Kopp [2011]
		111	−10.4	6.3		0.5		0.7		?		2	Heuret [2005], this study
		112	−10.7	6.1		0.2	0.2			?		2	Shulgin et al. [2011]
		113	−10.7	6.1		0.1	0.2			?		2	Kopp [2011]
		115	−11.2	6.7		0.2		0.1		?		2	Heuret [2005], this study
		116	−11.2	6.7		0.3	0			?		2	Kopp [2011], this study
	E-Java	117	−11.3	6.7		0.4		0		?		2	Heuret [2005], this study

(continued on next page)

Supplementary Table S1. (continued)

Region	Trench	Lon	Lat	Z_t	T_{SP}	T_{SP}^*	T_{sed}	T_{sed}^*	$T_{channel}$	$T_{channel}^*$	MT	MT*	Sources
	W-Timor	119	−11.1	6.5		C	0		C		NA		Kopp [2011]
	Timor	121	−12.1	3.8		C		C	C		NA		Kopp [2011]
		123	−11.2	1.8		C		C	C		NA		Heuret [2005], this study
		125	−10.2	2.2		C		C	C		NA		Heuret [2005], this study
		126.5	−9.6	2.8		C		C	C		NA		Heuret [2005], this study
	E-Timor	128.5	−9.2	3.0		C		C	C		NA		Heuret [2005], this study
	Tanimbar	130.5	−8.7	1.6		C		C	C		NA		Heuret [2005], this study
		132.5	−7.1	1.7		C		C	C		NA		Heuret [2005], this study
	Aru	133	−6.5	2		C	1.8		C		NA		Milsom et al. [1996]
		133	−5.2	1.3		C	1		C		NA		Milsom et al. [1996]
	W-Flores	117.2	−7.8	1.7		?	1.6			?		?	Silver et al. [1983]
	Flores	117.4	−7.8	1.7		?	1			?		?	Silver et al. [1983]
		118	−7.9	2.5		?		1.2		?		?	Heuret [2005], this study
		119	−7.8	3.7		?	1.2			?		?	Silver et al. [1983]
		120	−7.8	5.0		?		1.2		?		?	Heuret [2005], this study
		121	−7.8	3.9		?	1			?		?	Silver et al. [1983]
	E-Flores	122.7	−7.8	3.3		?	1			?		?	Silver et al. [1983]
	W-Wetar	124.9	−7.9	4.3		?	1.4			?		?	Silver et al. [1983]
	Wetar	126	−7.5	4.7		?		0.8		?		?	Heuret [2005], this study
	E-Wetar	127.1	−7.3	4		?	0.8			?		?	Silver et al. [1983]
	E-Seram	132	−3.4	1.9		C		2	C		NA		Heuret [2005], this study
	Seram	131.8	−3.2	1.5		C	2		C		NA		Pairault et al. [2003]
		131.2	−2.9	1.8		C	0.9		C		NA		Pairault et al. [2003]
		130	−2.4	2		C	0.9		C		NA		Pairault et al. [2003]
		128	−2.4	4.4		C			C		NA		Pairault et al. [2003]
	W-Seram	126	−2.7			C			C		NA		Heuret [2005], this study
	Halmahera	126.8	0	2.0									Heuret [2005]
		127.3	2	2.2									Heuret [2005]
	North_Sulawesi	123	2	5.9									Heuret [2005]
		121	2.3	5.4									Heuret [2005]

(continued on next page)

Supplementary Table S1. (continued)

Region	Trench	Lon	Lat	Z_t	T_{SP}	T_{SP}^*	T_{sed}	T_{sed}^*	$T_{channel}$	$T_{channel}^*$	MT	MT*	Sources
	N-Sangihe	126.4	1	2.4									Heuret [2005]
	Sangihe	127	3	2.0									Heuret [2005]
	S-Sangihe	126.6	5	3.6									Heuret [2005]
	S-Philippines	128.6	4	5.8									Heuret [2005]
	Philippines	127.4	6	8.9									Lallemand et al. [1998]
		127.3	8	8.9									Heuret [2005]
		126.8	10	9.8									Lallemand et al. [1998]
		126.2	12	7.7									Heuret [2005]
		125.2	14	6.3									Heuret [2005]
	N-Philippines	123.5	15.6	4.8									Heuret [2005]
	Cotobato	125.2	4.5	5.8									Heuret [2005]
		123.8	6.5	3.9									Heuret [2005]
	N-Sulu	121.7	10	3.9									Heuret [2005]
	Sulu	121.6	7.5	5.0									Heuret [2005]
	S-Sulu	119.7	6.5	4.0									Heuret [2005]
	S-Manila	119.2	14	−999		0.4		1.4		0.5		1	Heuret [2005], this study
	Manila	119.3	14.4	5.1	0.4		1.5			0.5	1		Hayes and Lewis [1984], this study
		119	15.3	5.1	0.3		1.3			0.5	1		Hayes and Lewis [1984], this study
		119.3	15.6	5.1	0.3		0.5		0.5		1		Hayes and Lewis [1984]
		119.2	16	5.1		0.3		0.7		0.5		1	Heuret [2005], this study
		119.2	16.3	4.6	0.4		0.9			0.4	1		Hayes and Lewis [1984], this study
		119.1	16.7	5		0.5	0.8		0.2		1		Hayes and Lewis [1984]
		119.2	17	4.1	0.7		1.7		0.3		1		Hayes and Lewis [1984]
		119.2	17.5	4.2		1		1.8		0.3		1	Heuret [2005], this study
		119.8	19	4.2		1.8		2		0		1	Heuret [2005], this study
		119.9	19.2	3.6	2		2		0		1		Eakin et al. [2014], Ku and Hsu [2009]
		120.1	19.4	4.1	2		2.2			0	1		Ku and Hsu [2009], this study
		120.2	19.7	4.1	2.3		2.6			0	1		Ku and Hsu [2009], this study
		120.3	20	4.1	2.2		3.2			0	1		Ku and Hsu [2009], this study
		120.3	20.2	4		2.1	1.1			0	1		Ku and Hsu [2009], this study

(continued on next page)

Supplementary Table S1. (continued)

Region	Trench	Lon	Lat	Z_t	T_{SP}	$T_{SP}{}^*$	T_{sed}	$T_{sed}{}^*$	$T_{channel}$	$T_{channel}{}^*$	MT	MT*	Sources
		120.3	20.4	4	2		0.8			0	1		Ku and Hsu [2009], this study
		120.2	20.5	3.9		1.7	1.8		0		1		Eakin et al. [2014]
		120.2	20.6	3.9	1.3		1.8			0	1		McIntosh et al. [2013], this study
		120.1	20.8	3.7	1.8		2.3			0	1		Ku and Hsu [2009], this study
		120	21	3.5	2		2			0	1		Ku and Hsu [2009], this study
		119.9	21.2	3.5		2.5	2		0		1		Lester et al. [2013]
		119.8	21.4	3.2	3		2.5		C		1		Eakin et al. [2014]
		119.9	22.5	1		3		2.5	C			1	Heuret [2005], this study
	N-Manila	120.5	24	−0.5		3		2.5	C			1	Heuret [2005], this study
	S-Ryukyus	122.5	23.2	5	1.5		4		0.5			1	Nishizawa et al. [2017], Okamura et al. [2017], Hsu et al. [2021], Lallemand et al. [2013], Deschamps et al. [2000]
	Ryukyus	123.1	23	6	0.5		4.5		1.7		1		Nishizawa et al. [2017], Okamura et al. [2017], Schnürle et al. [1998]
		124	23.2	6.6	0.2		1		0		2		Nishizawa et al. [2017], Okamura et al. [2017], Hsu et al. [2013]
		126.5	23.7	6.8	0.2		0.2			0	2		Park et al. [1998], Arai et al. [2016], this study
		127	24.2	7.2		0.2	0		0		2		Nishizawa et al. [2017], Okamura et al. [2017]
		127.5	25	7.3	0.2		1		0		2		Nishizawa et al. [2017], Okamura et al. [2017]
		129	25.7	7.1		0.2		0.4		0		2	Heuret [2005], this study
		130.5	27.5	5	0.2		0		0		2		Heuret [2005], this study
		131.7	28.7	4.5		0.2	0.2		0		2		Nishizawa et al. [2009], Arai et al. [2017], Nishizawa et al. [2017], Okamura et al. [2017]
		132	29.5	6	0.3		0.5		0			2	Nishizawa et al. [2009]
		132.5	30.5	4.3		0.2	0.1		0		2		Nishizawa et al. [2009]
	N-Ryukyus	133	31.1	5.3		0.2		0.1		0		2	Park et al. [2009], this study
	W-Nankai	133.9	31.7	4.8	0.7		1.6		0.5			1	Moore et al. [1990]
	Nankai	134	31.8	4.9		0.7	1.2			0.4		1	Park et al. [2002], this study
		135	32.2	4.8	0.8		1.3		0.5		1		Park et al. [2002, 2014], Kodaira et al. [2002], Park et al. [2000], Moore et al. [1990]
		135.5	32.6	4.7		0.8	1.6		0.2		1		Park and Kodaira [2012], Hamada et al. [2018]
		136.1	32.7	4.6	0.8		1.5		1		1		Park et al. [2009], Park and Kodaira [2012]
		137	33.1	4.3	0.7		1.3		0.6		1		Takahashi et al. [2002b], Park et al. [2002]
	E-Nankai	138	33.6	3		0.5	2.5		1.1			1	Mazzotti et al. [2002], Takahashi et al. [2002a]

(continued on next page)

Supplementary Table S1. (continued)

Region	Trench	Lon	Lat	Z_t	T_{SP}	T_{SP}^*	T_{sed}	T_{sed}^*	$T_{channel}$	$T_{channel}^*$	MT	MT*	Sources
	Suruga	138.5	34.1	3.7	0		2.8		0			NA	Górszczyk et al. [2019], Kodaira et al. [2004]
	Sagami	140	34.7	2.4		0		1.6		?		NA	Heuret [2005], this study
	N-Izu-Bonin	142.1	33	9.2		0.2		0.2		?		2	Heuret [2005], this study
	Izu-Bonin	142.2	32.2	9.1	0.2		0.2			?	2		Takahashi et al. [1998]
		142.2	31.3	9.7	0.3			0.3		?		2	Heuret [2005], this study
		142.3	31	9	0.3		0.3			?		2	Horine et al. [1990]
		142.9	29	8.9		0.3		0.3		?		2	Heuret [2005], this study
		143.3	27	8.8		0.3		0.3		?		2	Heuret [2005], this study
	S-Izu-Bonin	143.2	25	5.8		0.3		0.3		?		2	Heuret [2005], this study
	N-Mariana	145.1	23	7.0		0.3		0.3		?		2	Heuret [2005], this study
	Mariana	146.9	21	7.1		0.3		0.3		?		2	Heuret [2005], this study
		147.6	19	7		0.3		0.3		?		2	Heuret [2005], this study
		147.7	17.9	8.4	1		0.3			?	2		Oakley et al. [2008]
		147.8	17	8.4		1.5		0.6		0.6		2	Oakley et al. [2008], this study
		147.7	16.6	8.2	2		0.6		0.6		2		Oakley et al. [2008]
		147.6	16.4	6		1	0.3			?	2		Oakley et al. [2008]
		147.7	16.2	5.3	0.5			0.4		?		2	Oakley et al. [2008]
		147.5	15	8.5		0.5		0.4		0.5		2	Oakley et al. [2008], this study
		147.4	14.7	8.3	0.5		0.5		0.5			2	Oakley et al. [2008]
		147.3	14.5	9.2	0.5		0.3		0.3		2		Oakley et al. [2008]
		147.1	14	9.2		0.5		0.3		0.3		2	Oakley et al. [2008]
		146.5	13.3	8.7		0.5		0.3		0.3		2	Heuret [2005], this study
		144.5	12	9.6		0.5		0.3		?		2	Heuret [2005], this study
		142.5	11.4	10.7		0.5		0.3		?		2	Heuret [2005], this study
	S-Mariana	140.5	10.8	5.6		0.5		0.3		?		2	Heuret [2005], this study
	N-Yap	138.6	9.7	7.7	0.2		0.2			?	2		Dong et al. [2018], Yang et al. [2018], Zhang et al. [2019]
	Yap	138.2	9	5.3	0.3		0.2			?	2		Zhang et al. [2021]
		138	8.5	8.1	0.2		0.2			?	2		Zhang et al. [2021]
		138	8.6	7.9		0.2		0.2		?		2	Heuret [2005], this study
	S-Yap	136	7.3	6.2		0.2		0.2		?		2	Heuret [2005], this study
	Palau	134.5	6.8	6.9		0.2		0.2		?		2	Heuret [2005], this study

(continued on next page)

Supplementary Table S1. (continued)

Region	Trench	Lon	Lat	Z_t	T_{SP}	T_{SP}^*	T_{sed}	T_{sed}^*	$T_{channel}$	$T_{channel}^*$	MT	MT*	Sources
	W-New_Britain	148	−7.3	3.9									Heuret [2005]
	New_Britain	150	−7	7.0				0.5					Scholl et al. [2015]
	E-New_Britain	152	−6.1	8.2				0.5					Scholl et al. [2015]
	W-Solomons	154	−6.5	8.7									Heuret [2005]
	Solomons	156	−8	4.7									Heuret [2005]
		158	−9.3	4.0									Heuret [2005]
		160	−10.3	5.3									Heuret [2005]
		162	−11.3	7.6									Heuret [2005]
	E-Solomons	164	−11	7.3									Heuret [2005]
	N-New_Hebrides	165.7	−12	8.7		1		0.3		?		2	Heuret [2005], this study
	New_Hebrides	166.2	−14	6.1		0.4		1.4		1.4		2	Heuret [2005], this study
		166.3	−14.4	5.5		1	1.4		1.4		2		Fisher et al. [1986]
SOUTWEST PACIFIC		166.3	−14.7	4		0.8	1.1		1.2		2		Fisher et al. [1986]
		166.2	−15.1	5.4	0.7		1.9		1.9		2		Fisher et al. [1991]
		166.5	−15.6	3.9	1.3		1.9		2.6		2		Von Huene and Miller [1986], Fisher et al. [1991]
		166.4	−15.7	4	1		1.5		2		2		Fisher et al. [1986]
		166.6	−16	4.9	2			1.8		1.6		2	Heuret [2005], this study
		166.8	−16.2	4.6	0.6		2		1.2		2		Fisher et al. [1986]
		167.4	−17.2	6.4		0.5	2.5		1.3		2		Fisher et al. [1986]
		167.5	−17.5	6.7		0.3	0.4		1.5		2		Von Huene and Miller [1986]
		167.4	−17.6	6.7	0.2		0.4		1.6		2		Fisher et al. [1986]
		167.4	−18	6.8		0.2		0.4		1.6		2	Heuret [2005], this study
		168.2	−20	6.2		0.2		0.4		?		2	Heuret [2005], this study
		169.5	−22	6.1		0.2		0.4		?		2	Heuret [2005], this study
	S-New_Hebrides	171	−23	7.5		0.2		0.4		?		2	Heuret [2005], this study
	N-Tonga	187.7	−15.5	8.1		0.2		0.2		?		2	Wright et al. [2000]
	Tonga	187.8	−17	8.6		0.2		0.2		?		2	Wright et al. [2000]
		187.2	−19	8.4		0.2		0.2		?		2	Wright et al. [2000]
		186.5	−21	9.1		0.2		0.2		?		2	Heuret [2005], this study

(continued on next page)

Supplementary Table S1. (continued)

Region	Trench	Lon	Lat	Z_t	T_{SP}	$T_{SP}{}^*$	T_{sed}	$T_{sed}{}^*$	$T_{channel}$	$T_{channel}{}^*$	MT	MT*	Sources
		185.4	−23	10.5		0.2		0.2		?		2	Wright et al. [2000]
		184.9	−24.4	9	0.2		0.2			?	2		Contreras-Reyes et al. [2011]
		184.8	−24.5	9.3		0.2		0.4		?	2		Stratford et al. [2015]
		184.8	−25	8.1		0.2		0.8		0		2	Heuret [2005], this study
		184.8	−25.2	7.5		0.2	1.2			?		2	Ballance et al. [1989]
	S-Tonga	184.7	−25.8	5.9	0		0		0		2		Stratford et al. [2015]
	N-Kermadec	184.5	−26.7	8.4	0.7		0.2			?	2		Funnell et al. [2017]
	Kermadec	184.5	−27	8.6		0.5		0.4		0		2	Scholl et al. [2015], this study
		184.3	−27.7	9.4	0.4		0.8			?		2	Funnell et al. [2017]
		184.1	−27.9	9.6	0.2		1.3			?	2		Stratford et al. [2015]
		183.9	−29	8.5		0.2		0.4		?		2	Scholl et al. [2015]
		183.2	−31	8.5		0.2		0.4		?		2	Scholl et al. [2015]
		182.2	−33	8.8		0.2		0.4		?		2	Scholl et al. [2015]
		181.6	−35	7.3		0.2		0.4		?		2	Scholl et al. [2015]
		180.6	−36.5	4.9		0.2		0.4		?		2	Scholl et al. [2015]
		180.3	−37.1	5.2		0.2	0.5			?		2	Han et al. [2017]
	S-Kermadec	179.8	−37.8	3.7		0.5	2.3			?		1	Scherwath et al. [2010], Han et al. [2017]
	N-Hikurangi	179.5	−38	3.4		0.5		2.3		?		1	Barker et al. [2009]
	Hikurangi	179.1	−38.5	3.9		0.5		0.5		?		1	Heuret [2005], this study
		179	−38.8	3.3	0		0.7		0		1		Gase et al. [2021]
		179	−38.9	3.5	0		0.8		0		1		Barker et al. [2009], Bell et al. [2014, 2010], Barker et al. [2018]
		179	−39	3.5	1		0		0		1		Gase et al. [2021]
		178.8	−39.1	3.4		1	1.5		0		1		Gase et al. [2021]
		178.6	−39.9	3.3		1.5	5		2.5		1		Barker et al. [2009], Bell et al. [2010]

(continued on next page)

Supplementary Table S1. (continued)

Region	Trench	Lon	Lat	Z_t	T_{SP}	$T_{SP}{}^*$	T_{sed}	$T_{sed}{}^*$	$T_{channel}$	$T_{channel}{}^*$	MT	MT*	Sources
		178.7	−40	3.2		1.5		4.5		2		1	Heuret [2005], this study
		178.2	−40.6	3		2	3.3		0		1		Gase et al. [2022]
		178	−41	2.8		2.5	4.8		1.1		1		Von Huene and Miller [1986]
		178	−41.2	3		2.5	3		0.8		1		Gase et al. [2022]
		177.8	−41.3	2.9		2.5	5		1.3		1		Gase et al. [2022]
		177	−41.4	2.7		2.5		4.7		1		1	Heuret [2005], this study
		177.1	−41.5	2.9		3	4.5		0.8		1		Gase et al. [2022]
		175.8	−41.9	2.5		3	6			0.8	1		Lewis et al. [1998], this study
	S-Hikurangi	175	−42.3	2.6		3		6		0.8		1	Heuret [2005], this study
	N-Puysegur	166.1	−45.2	4.5	1.2		1.8		0.3			1	Lebrun et al. [2000]
	Puysegur	165.9	−45.7	4.5	0.8		3.5			0.5		1	Lebrun et al. [2000], this study
		165.4	−46	4.1		0.7	0.6			0.7		2	Lebrun et al. [2000], this study
		165	−46.3	5		0.7	2.2			1		2	Lebrun et al. [2000], this study
		165	−46.7	4.8	0.6		1.2		1.5			2	Lebrun et al. [2000], Delteil et al. [1996]
		164.8	−47.5	5.9		1	3			1.5		2	Lamarche and Lebrun [2000], this study
		164.8	−47.6	5.9	1.1		1.2			?		2	Lamarche and Lebrun [2000]
		164.5	−48	5.8		1		1		?		2	Heuret [2005], this study
	S-Puysegur	164	−49	5.9	0.8			0.8		?		2	Delteil et al. [1996]

lat-lon: intersection coordinates between trench and profile (generally normal to the trench); Z_t: trench depth measured on seismic profile; T_{SP}: mean sediment thickness measured along a seismic line away from the trench fill; $T_{SP}{}^*$: mean sediment thickness away from the trench fill, extrapolated from nearby observations; T_{sed}: maximum sediment thickness measured beneath the frontal thrust in the trench along a seismic line; $T_{sed}{}^*$: maximum sediment thickness beneath the frontal thrust in the trench extrapolated from nearby observations; $T_{channel}$: mean sediment thickness measured along a seismic line within the subduction channel; $T_{channel}{}^*$: mean sediment thickness within the subduction channel extrapolated from nearby observations; MT: margin type −1 for dominantly accretionary, 2 for dominantly erosional, during the last 1 Ma, along a seismic line; MT*: margin type −1 for dominantly accretionary, 2 for dominantly erosional, during the last 1 Ma, extrapolated from nearby observations; C: continental crust (sediment thickness is not measured).

2. Porosity and fluxes estimation

Estimating the mean porosity in the channel (hereafter labeled "porosity") is not trivial, as it depends on multiple factors such as the porosity of the sedimentary section prior to subduction, the permeability (or nature) of the medium and the subduction rate [e.g. Nikolinakou et al., 2023]. We have chosen to simplify the problem by considering that the porosity of the sediments dragged from the trench to the deeper channel, at an average distance of 15 km from the trench $\Phi_{channel}$ is equal to that of the subducted section at the deformation front Φ_{sed} multiplied by a constant reducing coefficient K_r.

$$\Phi_{channel} = K_r \times \Phi_{sed} \tag{1}$$

Similarly, the reduction in porosity during burial will have the effect of compacting the incoming section by a factor Kco, which simulates the fact that the amount of solid matter will be constant while that of fluid will be reduced.

$$T_{sed\_co} = K_{co} \times T_{sed}. \tag{2}$$

In the case of erosion or non-accretion, the thickness of the channel $T_{channel}$ is envisioned as being made of two layers: the deeper one is inherited from trench sediments having experienced compaction, while the upper one results from the margin erosion yielding channel thickening (Figure 4b). $T_{channel}$ is therefore equal to the thickness of the trench section T_{sed} compacted during its transit from the deformation front, i.e., T_{sed_co}, plus those of the eroded sediment from the overlying margin T_{ero}.

$$T_{channel} = T_{sed\_co} + T_{ero}. \tag{3}$$

In the case of accretion, only the basal section T_{sed_base} of the sedimentary pile at trench T_{sed} will be subducted (Figure 4a), characterized by a porosity: $\Phi_{sed\_base\_co}$, as aforementioned.

$$\Phi_{sed\_base\_co} = K_r \times \Phi_{sed\_base} \tag{4}$$

$$T_{channel} = K_{co} \times T_{sed\_base} \tag{5}$$

Expressing the solid mass conservation through compaction, and using Equation (4) we get:

$$K_{co} = (1 - \Phi_{sed\_base}) / (1 - K_r \times \Phi_{sed\_base}) \tag{6}$$

Thus, the estimate of $\Phi_{channel}$ will differ depending on whether the margin regime is erosive or accretionary. Indeed, in the case of frontal accretion, the porosity of the incoming section Φ_{sed_base} will be less than that of the average porosity at the trench Φ_{sed} (Figures S1 and S2), depending on its burial under T_{accret} (Figure 4), since porosity decreases significantly with depth. Conversely, in an erosive regime, some material with low porosity (because it is already compacted) will gradually be added to the input entire sedimentary section from the trench. This latter porosity is arbitrary set to 5%, i.e., equivalent to the porosity at trench under 10 km of sediment (see Figure S1).

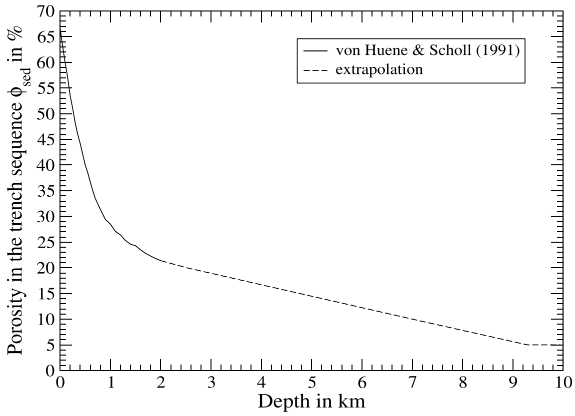

Supplementary Figure S1. Depth versus porosity curve of trench floor sedimentary deposits Φ_{sed} from Von Huene and Scholl [1991] extrapolated beyond 2 km.

We've used the average sediment porosity curve as a function of depth at trench provided by Von Huene and Scholl [1991]. As the values do not go beyond 2000 m, we have extrapolated them deeper to a plateau of 5% porosity at around 9200 m (Figure S1). From that depth versus porosity curve, we have estimated the mean porosity of the sediment section Φ_{sed} versus the sediment thickness T_{sed} and fit it with the dashed curve (Figure S3):

$$\Phi_{sed} = -11.3 \times \ln(T_{sed}/41.3) \text{ in percent} \tag{7}$$

We have calibrated the porosity reduction K_r, based on a seismic line off Ecuador, an erosive margin, near 2°S where Sage et al. [2006] have estimated $\Phi_{channel} \approx 28\%$ from the seismic velocities at a distance of ∼15 km from the deformation front, with $T_{channel}$ = 0.6 km, T_{sed} = 0.4 km, Φ_{ero} = 5%, Φ_{sed_base} = 54% and $\Phi_{sed\_base\_co}$ = 39.5%. We get $K_r \approx 0.85$.

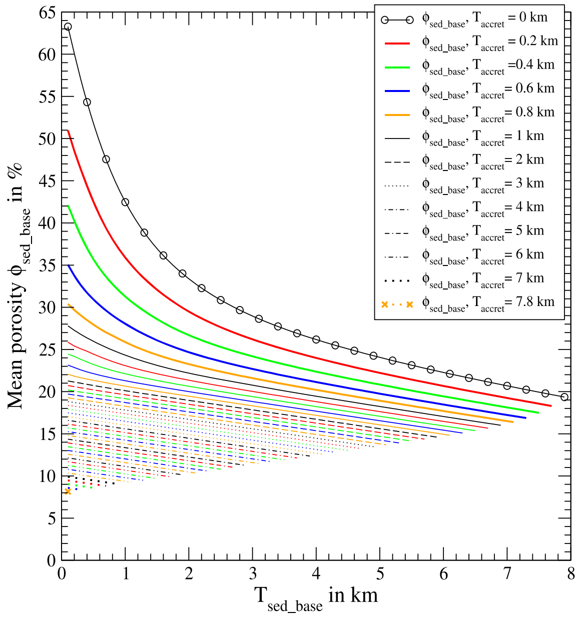

Supplementary Figure S2. Predicted mean porosity of the incoming sediment section at trench Φ_{sed_base} as a function of its thickness T_{sed_base} and those of the frontally accreted section T_{accret}. Curves are drawn for incremental loads at trench, every 0.2 km. The upper black one with circles represents the mean trench deposits porosity without frontal accretion Φ_{sed}.

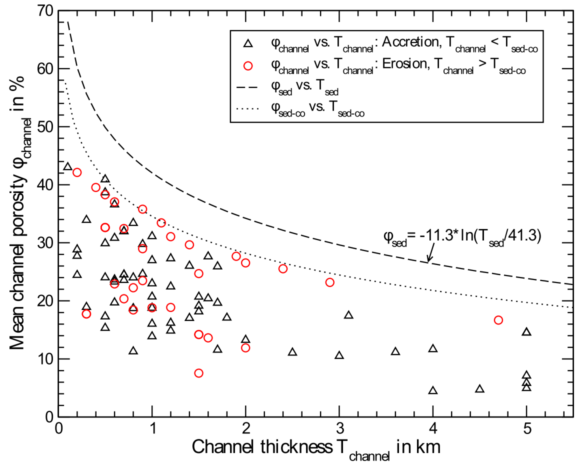

Supplementary Figure S3. Plot of mean channel porosity $\Phi_{channel}$ versus $T_{channel}$ along the 116 transects constrained by nearby seismic lines (see Table S2). Black triangles are values taken when frontal accretion occurs and red circles when subcrustal erosion is ongoing. The upper dashed curve is a reminder of the mean trench porosity Φ_{sed} versus trench sediment thickness T_{sed}, while the dotted curve represents Φ_{sed_co} versus T_{sed_co}, i.e., without frontal accretion.

In an idealized situation where the margin state would be neither accretionary nor erosional, we would expect that $T_{channel} = T_{sed\_co}$. The threshold used to distinguish whether we are in an accretionary or a non-accretionary case (potentially erosional) is thus obtained by comparing $T_{channel}$ to T_{sed_co} (Figure 4).

Based on our dataset and Figure S2, we were able to estimate Φ_{sed_base} in the accretion case ranging between 0.10 and 0.34. This allowed us to estimate the compaction coefficient $K_{co} \approx 0.95 \pm 0.03$.

Then, we calculated $\Phi_{channel}$ as:

$$\Phi_{channel} = 0.85 \times \Phi_{sed\_base}, \tag{8}$$

in the accretionary case and:

$$\Phi_{channel} = (\Phi_{sed\_co} \times T_{sed\_co} + 0.05 \times (T_{channel} - T_{sed\_co}))\,/\,T_{channel}, \tag{9}$$

in the non-accretionary case, with $\Phi_{sed\_co} = 0.85\Phi_{sed}$ (4) and where all porosities are now expressed as a volume fraction and not in percent.

To move from discrete data along the 535 seismic lines (Table S1) to data representative of each subduction zone (Table 3), we proceeded in 2 steps: (1) we projected the measurements (T_{sed}, $T_{channel}$) along the 260 transects listed in the submap database whenever we had the information on $T_{channel}$ to do so. We were thus able to provide 116 transects unevenly distributed over the 260 (see transects highlighted in green in Table S2), (2) the average $T_{channel}$ thickness is then split into a solid fraction and a liquid fraction based on the estimated porosity in the channel $\Phi_{channel}$, (3) the solid and liquid material fluxes in km^3/m·y/km of trench transiting the channel will therefore be the product of the related fraction and the normal component of the subduction velocity v_{sn} taken from the submap database. Thus, the material fluxes presented by subduction zone in Table 3 are extrapolated from values obtained along constrained transects (Table S2), weighted according to the widths sampled per transect.

Supplementary Table S2. Characteristic parameters of sediment fluxes for each submap transect

Short Name	Trench Name	Lon	Lat	Tsed (km)	Tsed* (km)	Tchannel (km)	Tchannel* (km)	Subduction rate normal component (mm/yr)	Sampling width (km)	Estimated porosity of channel sediment section 15 km landward of DF (%)	Solid fraction of channel sediment thickness 15 km landward of DF (km)	Fluid fraction of channel sediment thickness 15 km landward of DF (km)	Estimated solid fraction subducted (km3/m.y./km of trench)	Estimated fluid fraction subducted (km3/m.y./km of trench)
MED1	Calabria	17.4	40		7.0			2	200					
MED2	Calabria	19.2	37.6	7.0		2.5		9	254	11.1	2.22	0.28	20.0	2.5
MED3	Calabria	18	36.1	4.3		3.1		11	200	17.4	2.56	0.54	28.2	5.9
MED4	Aegean	18.8	37	6.5			5.0	18	150	14.5	4.27	0.73	76.9	13.1
MED5	Aegean	18.9	35		6.5		5.0	34	199	14.5	4.27	0.73	145.2	24.8
MED6	Aegean	20	33.7		10.5		5.0	38	185	7.1	4.64	0.36	176.3	13.7
MED7	Aegean	22	33.2		11.5	5.0		40	191	5.9	4.71	0.29	188.4	11.6
MED8	Aegean	24	33		12.5		5.0	40	198	5.0	4.75	0.25	190.0	10.0
MED9	Aegean	26	32.2		12.5		4.5	34	207	4.7	4.29	0.21	145.9	7.1
MED10	Aegean	28	33	12.5		4.0		37	225	4.4	3.82	0.18	141.3	6.7
MED11	Aegean	30	34.4		9.5			14	191					
MED12	Cyprean	31.5	34.6		9.0			14	166					
MED13	Cyprean	33.5	34.1	7.2				10	220					
MED14	Makran	57.5	24.7		7.3			29	120					
MED15	Makran	59.5	24.2	3.0		4.7		30	207	16.7	3.92	0.78	117.6	23.4
MED16	Makran	61.5	24		7.4		4.0	29	204	11.7	3.53	0.47	102.4	13.6
MED17	Makran	63.5	24.1	7.5		3.6		30	205	11.2	3.20	0.40	96.0	12.0
MED18	Makran	65.5	24.5		7.5		3.0	27	200	10.5	2.69	0.31	72.6	8.4
NPA1	Japan	142.2	35		0.5	1.2		93	240	18.9	0.97	0.23	90.2	21.4
NPA2	Japan	143.5	37	0.4		1.5		92	241	14.2	1.29	0.21	118.3	19.7
NPA3	Japan	144.2	39		0.4	2.0		89	200	11.9	1.76	0.24	156.8	21.2
NPA4	Japan	144.5	40.5		0.4	1.0		92	154	18.8	0.81	0.19	74.6	17.4
NPA5	Kurils	145.5	41.5		0.8		0.6	82	143	36.6	0.38	0.22	31.2	18.0
NPA6	Kurils	147	42.2		0.4	0.4		78	182	39.5	0.24	0.16	18.8	12.4
NPA7	Kurils	149	43.5		0.4		0.5	82	203	32.6	0.34	0.16	27.6	13.4
NPA8	Kurils	151	44.4	0.4				74	188					
NPA9	Kurils	153	45.3		0.4			82	218					
NPA10	Kurils	155.1	47		0.4		0.5	86	267	32.6	0.34	0.16	28.9	14.1
NPA11	Kurils	157.5	49		0.5	0.5		83	290	38.3	0.31	0.19	25.8	15.7
NPA12	Kamchatka	160.2	51		0.6		0.5	84	280	42.7	0.29	0.21	24.4	17.6
NPA13	Kamchatka	162.3	53	0.6				82	213					
NPA14	Kamchatka	163.4	54.3	2.0				81	200					
NPA15	Aleutians	165	54.9		1.0			-5	160					
NPA16	Aleutians	167	53.8		2.0			3	172					
NPA17	Aleutians	169	52.9		2.0			9	164					
NPA18	Aleutians	171	52.1		2.0			14	155					
NPA19	Aleutians	173	51.6		2.0			19	149					
NPA20	Aleutians	175	51.1		2.0			33	147					
NPA21	Aleutians	177	50.8		1.5			33	146					
NPA22	Aleutians	179	50.4		1.5			43	145					
NPA23	Aleutians	181	50.3		2.0			59	142					
NPA24	Aleutians	183	50.4		2.0		1.2	66	142	22.5	0.93	0.27	61.4	17.8
NPA25	Aleutians	185	50.5	1.2		1.1		65	143	33.4	0.73	0.37	47.5	24.1
NPA26	Aleutians	187	50.8	3.0			1.5	64	144	18.2	1.23	0.27	78.7	17.3
NPA27	Aleutians	189	51.1		2.0		1.9	69	145	27.7	1.37	0.53	94.5	36.6
NPA28	Aleutians	191	51.5		2.0			69	147					
NPA29	Aleutians	193	52		2.0			68	148					
NPA30	Aleutians	195	52.5		1.0			67	149					
NPA31	Alaska	197	53.1	0.9				66	145					
NPA32	Alaska	199	53.5		1.2		1.0	63	138	31.1	0.69	0.31	43.5	19.5
NPA33	Alaska	201	53.8		1.5		0.9	62	137	24.6	0.68	0.22	42.2	13.6
NPA34	Alaska	203	54.2	1.0		0.8		61	142	33.4	0.53	0.27	32.3	16.5
NPA35	Alaska	205	54.8		1.7		1.0	58	150	23.0	0.77	0.23	44.7	13.3
NPA36	Alaska	207	55.6		2.0		1.7	52	148	25.9	1.26	0.44	65.5	22.9
NPA37	Alaska	209	56.2		2.7		1.7	52	150	19.7	1.37	0.33	71.2	17.2
NPA38	Alaska	211	57.1		2.6		1.5	47	157	19.1	1.21	0.29	56.9	13.6
NPA39	Alaska	213	58		2.5		1.6	46	153	20.4	1.27	0.33	58.4	15.2
NPA40	Alaska	214.5	59.1		2.0		2.0	41	89	26.5	1.47	0.53	60.3	21.7
NPA41	Alaska	215	59.1		2.0			14	30					
NPA42	Alaska	215.5	59.2	2.7		0.0		19	40					0.0
NPA43	Cascadia	231.7	50		2.8			41	260					
NPA44	Cascadia	233.4	48		3.0		0.5	37	245	17.3	0.41	0.09	15.2	3.3
NPA45	Cascadia	234.4	46		3.5	0.0		30	229					0.0
NPA46	Cascadia	234.6	44		3.5		1.8	23	223	17.1	1.49	0.31	34.3	7.1
NPA47	Cascadia	234.7	42		3.5			20	230					
SAM1	C-America	254.5	19.1		0.7			51	210					
SAM2	C-America	256	17.9		0.7			63	223					
SAM3	C-America	258	16.9		0.7			67	231					
SAM4	C-America	260	16.3		0.7			69	225					
SAM5	C-America	262	15.6		0.7			71	222					
SAM6	C-America	264	15.3		0.7			70	232					
SAM7	C-America	266	14.2		0.7			74	245					
SAM8	C-America	268	13.2		0.7			79	241					
SAM9	C-America	270	12.3		0.6			77	239					
SAM10	C-America	272	11.4		0.6		0.7	75	276	32.5	0.47	0.23	35.3	17.3
SAM11	C-America	274	9.4	0.7		0.9		67	279	29.0	0.64	0.26	42.9	17.4
SAM12	C-America	276	8.4		1.4		1.0	70	270	27.0	0.73	0.27	51.1	18.9
SAM13	Panama	279	10		2.0			10	170					
SAM14	Panama	280.5	10.5		2.0			11	169					
SAM15	Panama	282	10.4		2.0			9	180					
SAM16	Venezuela	283.5	10	4.0		0.0		3	232					0.0
SAM17	Venezuela	285	12.2		4.0			4	274					
SAM18	Venezuela	287	13.4		1.8			2	238					
SAM19	Venezuela	289	13.8		1.8			0	220					
SAM20	Venezuela	291	13.5	1.8			1.4	-1	220	26.0	1.04	0.36	-1.0	-0.4
SAM21	Venezuela	293	13.1		3.8		1.2	-2	220	16.2	1.01	0.19	-2.0	-0.4
SAM22	Muertos	290	17.3	0.3		0.1		6	210	43.3	0.06	0.04	0.4	0.2
SAM23	Muertos	292	17.2	1.5		0.7		2	213	23.6	0.53	0.17	1.1	0.3
SAM24	Muertos	294	17.2	1.3		0.7		1	200	24.5	0.53	0.17	0.5	0.2
SAM25	Hispaniola	290	20		2.5			1	200					
SAM26	Puerto-Rico	292	19.6	1.0				3	212					
SAM27	Puerto-Rico	294	19.8		2.0			4	210					
SAM28	Antilles	296	19.8	0.2			0.2	8	213	42.1	0.12	0.08	1.0	0.6
SAM29	Antilles	298	19.3	0.1		0.3		13	228	17.8	0.25	0.05	3.3	0.7
SAM30	Antilles	299.8	18	0.8		0.3		18	253	33.9	0.20	0.10	3.6	1.8
SAM31	Antilles	301.2	16	1.0		0.6		20	260	30.8	0.41	0.19	8.2	3.8
SAM32	Antilles	302.3	14		5.5		2.0	20	238	13.3	1.73	0.27	34.6	5.4
SAM33	Antilles	302.6	12	6.3		1.7		18	240	11.6	1.50	0.20	27.0	3.6

Supplementary Table S2. (continued)

SAM34	Andean	281.9	5		1.0		0.5	41	240	29.9	0.35	0.15	14.4	6.2
SAM35	Andean	280.9	3.5	1.8		0.6		38	200	19.7	0.48	0.12	18.2	4.6
SAM36	Andean	279.9	2	3.5		1.0		42	222	16.0	0.84	0.16	35.3	6.7
SAM37	Andean	279	0		0.3		0.6	48	237	22.9	0.46	0.14	22.1	6.7
SAM38	Andean	278.5	-2		0.3		0.7	51	228	20.4	0.56	0.14	28.3	7.4
SAM39	Andean	278.1	-4		1.0		0.9	55	197	35.8	0.58	0.32	31.9	17.6
SAM40	Andean	278.1	-5.5	1.3		0.7		62	168	24.5	0.53	0.17	32.9	10.5
SAM41	Andean	278.4	-7		1.0		0.7	64	205	32.0	0.48	0.22	30.7	14.1
SAM42	Andean	279.2	-9	1.0			0.7	63	249	32.0	0.48	0.22	30.2	13.9
SAM43	Andean	280.4	-11	0.3			0.8	63	261	18.4	0.65	0.15	41.0	9.4
SAM44	Andean	281.7	-13		0.3		0.8	62	276	22.3	0.62	0.18	38.5	11.1
SAM45	Andean	283.4	-15		0.3			60	318					
SAM46	Andean	285.9	-17		0.2			47	331					
SAM47	Andean	288	-19		0.2		1.5	56	274	14.2	1.29	0.21	72.0	12.0
SAM48	Andean	288.7	-21		0.1		1.5	57	228	7.6	1.39	0.11	79.2	6.3
SAM49	Andean	288.7	-23		0.1		0.3	65	223	17.8	0.25	0.05	16.3	3.3
SAM50	Andean	288.6	-25		0.1			66	224					
SAM51	Andean	288.3	-27		0.1			62	227					
SAM52	Andean	287.7	-29	0.2				63	199					
SAM53	Andean	287.5	-30.5	0.3				66	167					
SAM54	Andean	287.4	-32	0.5			0.9	65	197	23.5	0.69	0.21	44.9	13.6
SAM55	Andean	286.9	-34	1.2			0.9	53	203	29.8	0.63	0.27	33.4	14.3
SAM56	Andean	286.2	-35.5	2.0		1.0		49	180	20.7	0.79	0.21	38.7	10.3
SAM57	Andean	285.4	-37		2.1		0.8	65	204	18.7	0.65	0.15	42.3	9.8
SAM58	Andean	284.9	-39	1.6		1.2		68	225	27.3	0.87	0.33	59.2	22.4
SAM59	Andean	284.7	-41	2.4			1.0	69	223	18.8	0.81	0.19	55.9	13.1
SAM60	Andean	284.5	-43	2.4		1.5		69	225	20.7	1.19	0.31	82.1	21.4
SAM61	Andean	283.9	-45	1.1			1.5	69	225	24.7	1.13	0.37	78.0	25.5
SAM62	Andean	283.8	-47	1.2			1.2	20	229	31.1	0.83	0.37	16.6	7.4
SAM63	Andean	282.8	-49	1.5				19	230					
SAM64	Andean	283.3	-51		2.8		2.9	18	226	23.2	2.23	0.67	40.1	12.1
SAM65	Andean	283.9	-53	2.5			2.4	18	239	25.5	1.79	0.61	32.2	11.0
SAM66	Andean	285.7	-55	3.4			1.4	13	300	17.1	1.16	0.24	15.1	3.1
SAM67	Sandwich	329	-54.8		0.9			5	150					
SAM68	Sandwich	331	-54.9		0.9			11	129					
SAM69	Sandwich	333	-55.1		0.9			38	143					
SAM70	Sandwich	334.9	-56		0.9			65	196					
SAM71	Sandwich	336.2	-58		0.5			72	231					
SAM72	Sandwich	335.4	-60		0.5			37	160					
SEA1	Andaman	92.1	14	2.2				13	240					
SEA2	Andaman	91.6	12		2.4		0.0	22	226					0.0
SEA3	Andaman	91.4	10	2.6		0.0		31	224					0.0
SEA4	Andaman	91.7	8		3.4		0.0	37	234					0.0
SEA5	Andaman	92.6	6		4.1			44	235					
SEA6	Sumatra	93	4	4.3				49	271					
SEA7	Sumatra	95	2	3.5				41	314					
SEA8	Sumatra	97	0		2.5			43	284					
SEA9	Sumatra	98.1	-2	0.8				48	269					
SEA10	Sumatra	99.7	-4		1.3		0.0	51	246					0.0
SEA11	Sumatra	100.8	-5.5	0.8		0.0		53	221					0.0
SEA12	Sumatra	102.3	-7	1.1			0.2	56	285	28.9	0.14	0.06	7.8	3.4
SEA13	Java	105	-8.4		1.5		0.6	61	299	23.3	0.46	0.14	28.1	8.5
SEA14	Java	107	-9.7		1.5		0.8	65	250	24.0	0.61	0.19	39.7	12.4
SEA15	Java	109	-10.5		1.2			67	228					
SEA16	Java	111	-10.4		0.7			67	220					
SEA17	Java	113	-10.7	0.2				65	223					
SEA18	Java	115	-11.2		0.1			62	222					
SEA19	Java	117	-11.3		0.0			55	219					
SEA20	Timor	119	-11.1					45	232					
SEA21	Timor	121	-12.1					26	242					
SEA22	Timor	123	-11.2					14	242					
SEA23	Timor	125	-10.2					14	211					
SEA24	Timor	126.5	-9.6					9	201					
SEA25	Timor	128.5	-9.2					4	225					
SEA26	Tanimbar	130.5	-8.7					0	255					
SEA27	Tanimbar	132.5	-7.1					-1	251					
SEA28	Aru	133.0	-5.2	1.0				-28	220					
SEA29	Flores	118	-7.9		1.2			20	285					
SEA30	Flores	120	-7.8		1.2			30	285					
SEA31	Wetar	126	-7.5		0.8			27	350					
SEA32	Seram	132	-3.4		2.0			48	250					
SEA33	Seram	130	-2.4	0.9				10	235					
SEA34	Seram	128	-2.4					-5	220					
SEA35	Halmahera	126.8	0					43	350					
SEA36	Halmahera	127.3	2					36	350					
SEA37	N-Sulawesi	123	2					18	220					
SEA38	N-Sulawesi	121	2.3					34	220					
SEA39	Sangihe	126.4	1					47	350					
SEA40	Sangihe	127	3					43	229					
SEA41	Sangihe	126.6	5					38	350					
SEA42	Philippines	128.6	4		0.4			21	240					
SEA43	Philippines	127.4	6		0.4			27	241					
SEA44	Philippines	127.3	8		0.4			36	226					
SEA45	Philippines	126.8	10		0.4			32	230					
SEA46	Philippines	126.2	12	0.2				41	240					
SEA47	Philippines	125.2	14		0.4			24	251					
SEA48	Philippines	123.5	15.6	0.5				8	240					
SEA49	Cotobato	125.2	4.5					-999	190					
SEA50	Cotobato	123.8	6.5					17	190					
SEA51	Sulu	121.7	10					52	200					
SEA52	Sulu	121.6	7.5					27	270					
SEA53	Sulu	119.7	6.5					11	200					
SEA54	Manila	119.2	14		1.4		0.5	45	200	24.0	0.38	0.12	17.1	5.4
SEA55	Manila	119.2	16		0.7		0.5	63	195	38.7	0.31	0.19	19.5	12.0
SEA56	Manila	119.2	17.5		1.8		0.3	73	173	18.9	0.24	0.06	17.5	4.4
SEA57	Manila	119.8	19		2.0		0.0	83	175					0.0
SEA58	Manila	120.2	20.5	1.8		0.0		-999	198					0.0
SEA59	Manila	119.9	22.5		2.5			46	201					
SEA60	Manila	120.5	24		2.5			35	200					
SEA61	Ryukyus	122.5	23.2	4.0		0.5		66	150	15.3	0.42	0.08	27.7	5.3
SEA62	Ryukyus	124	23.2	1.0		0.0		109	239					0.0
SEA63	Ryukyus	127	24.2	0.0		0.0		114	293					0.0
SEA64	Ryukyus	129	25.7		0.4		0.0	102	256					0.0
SEA65	Ryukyus	130.5	27.5	0.0		0.0		92	258					0.0
SEA66	Ryukyus	132	29.5	0.5		0.0		75	234					0.0

Supplementary Table S2. (continued)

SEA67	Ryukyus	133	31.1		0.1		0.0	45	162					0.0
SEA68	Nankai	134	31.8	1.2			0.2	37	145	27.7	0.14	0.06	5.2	2.2
SEA69	Nankai	135.5	32.6	1.6		0.2		33	159	24.4	0.15	0.05	5.0	1.7
SEA70	Nankai	137	33.1	1.3		0.6		30	164	23.7	0.46	0.14	13.8	4.2
SEA71	Suruga	138.5	34.1	2.8		0.0		18	165					0.0
SEA72	Sagami	140	34.7		1.6		NA	19	212					
SEA73	Izu-Bonin	142.1	33		0.2			53	247					
SEA74	Izu-Bonin	142.3	31	0.3				46	226					
SEA75	Izu-Bonin	142.9	29		0.3			38	228					
SEA76	Izu-Bonin	143.3	27		0.3			38	224					
SEA77	Izu-Bonin	143.2	25		0.3			31	259					
SEA78	Mariana	145.1	23		0.3			30	292					
SEA79	Mariana	146.9	21		0.3			41	262					
SEA80	Mariana	147.6	19		0.3			51	229					
SEA81	Mariana	147.8	17		0.6		0.6	55	224	37.0	0.38	0.22	21.0	12.0
SEA82	Mariana	147.5	15		0.4		0.5	55	221	32.6	0.34	0.16	18.5	9.0
SEA83	Mariana	146.5	13.3		0.3			43	239					
SEA84	Mariana	144.5	12		0.3			27	244					
SEA85	Mariana	142.5	11.4		0.3			9	228					
SEA86	Mariana	140.5	10.8		0.3			4	240					
SEA87	Yap	138.6	10	0.2				9	210					
SEA88	Yap	138	8.6		0.2			6	216					
SEA89	Yap	136	7.3		0.2			3	219					
SEA90	Palau	134.5	6.8		0.2			1	200					
SWP1	New Britain	148	-7.3	2.5				57	220					
SWP2	New Britain	150	-7		0.5			81	233					
SWP3	New Britain	152	-6.1		0.5			119	234					
SWP4	Solomons	154	-6.5	0.1				77	251					
SWP5	Solomons	156	-8	0.1				104	270					
SWP6	Solomons	158	-9.3	0.1				71	254					
SWP7	Solomons	160	-10.3		0.7			59	245					
SWP8	Solomons	162	-11.3	1.3				33	233					
SWP9	Solomons	164	-11		0.7			10	218					
SWP10	N-Hebrides	165.7	-12		0.3			91	222					
SWP11	N-Hebrides	166.2	-14		1.4		1.4	40	228	29.7	0.98	0.42	39.2	16.8
SWP12	N-Hebrides	166.6	-16		1.8		1.6	46	232	27.6	1.16	0.44	53.4	20.2
SWP13	N-Hebrides	167.4	-18		0.4		1.6	113	238	13.6	1.38	0.22	156.1	24.7
SWP14	N-Hebrides	168.2	-20		0.4			154	249					
SWP15	N-Hebrides	169.5	-22		0.4			103	225					
SWP16	N-Hebrides	171	-23		0.4			52	250					
SWP17	Tonga	187.7	-15.5		0.2			171	180					
SWP18	Tonga	187.8	-17		0.2			228	199					
SWP19	Tonga	187.2	-19		0.2			191	233					
SWP20	Tonga	186.5	-21		0.2			154	242					
SWP21	Tonga	185.4	-23		0.2			114	240					
SWP22	Tonga	184.8	-25		0.8		0.0	124	227					0.0
SWP23	Kermadec	184.5	-27		0.4		0.0	114	227					0.0
SWP24	Kermadec	183.9	-29		0.4			103	231					
SWP25	Kermadec	183.2	-31		0.4			91	237					
SWP26	Kermadec	182.2	-33		0.4			80	235					
SWP27	Kermadec	181.6	-35		0.4			69	209					
SWP28	Kermadec	180.6	-36.5		0.4			60	224					
SWP29	Hikurangi	179.1	-38.5		0.5		0.0	49	215					0.0
SWP30	Hikurangi	178.7	-40		4.5		1.2	40	191	14.9	1.02	0.18	40.8	7.2
SWP31	Hikurangi	177	-41.4		4.7		1.0	12	203	13.9	0.86	0.14	10.3	1.7
SWP32	Hikurangi	175	-42.3		6.0		0.8	10	160	11.3	0.71	0.09	7.1	0.9
SWP33	Puysegur	164.5	-48		1.0			25	350					

Underlined in green are the 116 transects (among 260) for which we have an estimate of T_{channel}. *means that the value is extrapolated from a nearby seismic line. DF means deformation front.

References

Agudelo, W., Ribodetti, A., Collot, J. Y., and Operto, S. (2009). Joint inversion of multichannel seismic reflection and wide-angle seismic data: Improved imaging and refined velocity model of the crustal structure of the North Ecuador–South Colombia convergent margin. *J. Geophys. Res.: Solid Earth*, 114(B2), article no. B02306.

Arai, R., Kodaira, S., Yamada, T., Takahashi, T., Miura, S., Kaneda, Y., Nishizawa, A., and Oikawa, M. (2017). Subduction of thick oceanic plateau and high-angle normal-fault earthquakes intersecting the slab. *Geophys. Res. Lett.*, 44(12), 6109–6115.

Arai, R., Takahashi, T., Kodaira, S., Kaiho, Y., Nakanishi, A., Fujie, G., Nakamura, Y., Yamamoto, Y., Ishihara, Y., Miura, S., and Kaneda, Y. (2016). Structure of the tsunamigenic plate boundary and low-frequency earthquakes in the southern Ryukyu Trench. *Nat. Commun.*, 7(1), article no. 12255.

Ballance, P. F., Scholl, D. W., Vallier, T. L., Stevenson, A. J., Ryan, H., and Herzer, R. H. (1989). Subduction of a Late Cretaceous seamount of the Louisville Ridge at the Tonga Trench: A model of normal and accelerated tectonic erosion. *Tectonics*, 8(5), 953–962.

Baranov, B. V., Tsukanov, N. V., Gaedicke, C., Freitag, R., and Dozorova, K. A. (2022). Morphology and structural features of the subduction zone in the vicinity of Kuril–Kamchatka–Aleutian junction. *Oceanology*, 62(4), 528–539.

Barker, D. H. N., Henrys, S., Caratori Tontini, F., Barnes, P. M., Bassett, D., Todd, E., and Wallace, L. (2018). Geophysical constraints on the relationship between seamount subduction, slow slip, and tremor at the north Hikurangi subduction zone, New Zealand. *Geophys. Res. Lett.*, 45(23), 12–804.

Barker, D. H. N., Sutherland, R., Henrys, S., and Bannister, S. (2009). Geometry of the Hikurangi subduction thrust and upper plate, North Island, New Zealand. *Geochem. Geophys. Geosyst.*, 10(2), article no. Q02007.

Bartolomé, R., Dañobeitia, J., Michaud, F., Córdoba, D., and Delgado-Argote, L. A. (2011). Imaging the seismic crustal structure of the western Mexican margin between 19°N and 21°N. *Pure Appl. Geophys.*, 168, 1373–1389.

Bell, R., Holden, C., Power, W., Wang, X., and Downes, G. (2014). Hikurangi margin tsunami earthquake generated by slow seismic rupture over a subducted seamount. *Earth Planet. Sci. Lett.*, 397, 1–9.

Bell, R., Sutherland, R., Barker, D. H. N., Henrys, S., Bannister, S., Wallace, L., and Beavan, J. (2010). Seismic reflection character of the Hikurangi subduction interface, New Zealand, in the region of repeated Gisborne slow slip events. *Geophys. J. Int.*, 180(1), 34–48.

Boucard, M., Marcaillou, B., Lebrun, J.-F., Laurencin, M., Klingelhoefer, F., Laigle, M., Lallemand, S., Schenini, L., Graindorge, D., Cornée, J.-J., Münch, P., Philippon, M., and the AntiTheSis and GARAnti Scientific teams (2021). Paleogene V-shaped basins and Neogene subsidence of the Northern Lesser Antilles Forearc. *Tectonics*, 40(3), article no. e2020TC006524.

Brocher, T. M., Fuis, G. S., Fisher, M. A., Plafker, G., Moses, M. J., Taber, J. J., and Christensen, N. I. (1994). Mapping the megathrust beneath the northern Gulf of Alaska using wide-angle seismic data. *J. Geophys. Res.: Solid Earth*, 99(B6), 11663–11685.

Cernobori, L., Hirn, A., McBride, J. H., Nicolich, R., Petronio, L., and Romanelli, M. (1996). Crustal image of the Ionian basin and its Calabrian margins. *Tectonophysics*, 264(1–4), 175–189.

Chamot-Rooke, N., Rangin, C., and Le Pichon, X. (2005). *DOTMED (Deep Offshore Tectonics of the Mediterranean): A Synthesis of Deep Marine Data in the Eastern Mediterranean.* Mémoires de la Société Géologique de France, Paris, 177. 64 p., 9 plates + CD.

Chaumillon, E. and Mascle, J. (1997). From foreland to forearc domains: new multichannel seismic reflection survey of the Mediterranean Ridge accretionary complex (Eastern Mediterranean). *Mar. Geol.*, 138(3–4), 237–259.

Collot, J. Y., Agudelo, W., Ribodetti, A., and Marcaillou, B. (2008). Origin of a crustal splay fault and its relation to the seismogenic zone and underplating at the erosional north Ecuador–south Colombia oceanic margin. *J. Geophys. Res.: Solid Earth*, 113(B12), article no. B12102.

Collot, J. Y., Marcaillou, B., Sage, F., Michaud, F., Agudelo, W., Charvis, P., Graindorge, D., Gutscher, M.-A., and Spence, G. (2004). Are rupture zone limits of great subduction earthquakes controlled by upper plate structures? Evidence from multichannel seismic reflection data acquired across the northern Ecuador–southwest Colombia margin. *J. Geophys. Res.: Solid Earth*, 109(B11), article no. B11103.

Collot, J. Y., Ribodetti, A., Agudelo, W., and Sage, F. (2011). The South Ecuador subduction channel: Evidence for a dynamic mega-shear zone from 2D fine-scale seismic reflection imaging and implications for material transfer. *J. Geophys. Res.: Solid Earth*, 116(B11), article no. B11102.

Collot, J. Y., Sanclemente, E., Nocquet, J. M., Leprêtre, A., Ribodetti, A., Jarrin, P., Chlieh, M., Graindorge, D., and Charvis, P. (2017). Subducted oceanic relief locks the shallow megathrust in central Ecuador. *J. Geophys. Res.: Solid Earth*, 122(5), 3286–3305.

Contreras-Reyes, E., Flueh, E. R., and Grevemeyer, I. (2010). Tectonic control on sediment accretion and subduction off south central Chile: Implications for coseismic rupture processes of the 1960 and 2010 megathrust earthquakes. *Tectonics*, 29(6), article no. TC6018.

Contreras-Reyes, E., Grevemeyer, I., Flueh, E. R., Scherwath, M., and Heesemann, M. (2007). Alteration of the subducting oceanic lithosphere at the southern central Chile trench–outer rise. *Geochem. Geophys. Geosyst.*, 8(7), article no. Q07003.

Contreras-Reyes, E., Grevemeyer, I., Watts, A. B., Flueh, E. R., Peirce, C., Moeller, S., and Papenberg, C. (2011). Deep seismic structure of the Tonga subduction zone: Implications for mantle hydration, tectonic erosion, and arc magmatism. *J. Geophys. Res.: Solid Earth*, 116(B10), article no. B10103.

Contreras-Reyes, E. and Osses, A. (2010). Lithospheric flexure modelling seaward of the Chile trench: implications for oceanic plate weakening in the Trench Outer Rise region. *Geophys. J. Int.*, 182(1), 97–112.

Davis, E. E., Hyndman, R. D., and Villinger, H. (1990). Rates of fluid expulsion across the Northern Cascadia Accretionary Prism: Constraints from new heat row and multichannel seismic reflection data. *J. Geophys. Res.: Solid Earth*, 95(B6), 8869–8889.

Delteil, J., Collot, J. Y., Wood, R., Herzer, R., Calmant, S., Christoffel, D., Coffin, M., Ferrière, J., Lamarche, G., Lebrun, J.-F., Mauffret, A., Pontoise, B., Popoff, M., Ruellan, E., Sosson, M., and Sutherland, R. (1996). From strike-slip faulting to oblique subduction: a survey of the Alpine Fault-Puysegur Trench transition, New Zealand, results of cruise Geodynz-sud leg 2. *Mar. Geophys. Res.*, 18(2–4), 383–399.

Deschamps, A., Monié, P., Lallemand, S., Hsu, S. K., and Yeh, K. Y. (2000). Evidence for early cretaceous oceanic crust trapped in the Philippine sea plate. *Earth Planet. Sci. Lett.*, 179(3–4), 503–516.

Deville, E. and Mascle, A. (2012). The Barbados ridge: A mature accretionary wedge in front of the Lesser Antilles active margin. In *Regional Geology and Tectonics: Principles of Geologic Analysis*, pages 580–607. Elsevier.

Dong, D., Zhang, Z., Bai, Y., Fan, J., and Zhang, G. (2018). Topographic and sedimentary features in the Yap subduction zone and their implications for the Caroline Ridge subduction. *Tectonophysics*, 722, 410–421.

Eakin, D. H., McIntosh, K. D., Van Avendonk, H. J. A., Lavier, L., Lester, R., Liu, C. S., and Lee, C. S. (2014). Crustal-scale seismic profiles across the Manila subduction zone: The transition from intraoceanic subduction to incipient collision. *J. Geophys. Res.: Solid Earth*, 119(1), 1–17.

Fisher, M. A., Collot, J. Y., and Geist, E. L. (1991). Structure of the collision zone between Bougainville Guyot and the accretionary wedge of the New Hebrides island arc, southwest Pacific. *Tectonics*, 10(5), 887–903.

Fisher, M. A., Collot, J. Y., and Smith, G. L. (1986). Possible causes for structural variation where the New Hebrides island arc and the d'Entrecasteaux zone collide. *Geology*, 14(11), 951–954.

Franke, D., Schnabel, M., Ladage, S., Tappin, D. R., Neben, S., Djajadihardja, Y. S., Müller, C., Kopp, H., and Gaedicke, C. (2008). The great Sumatra–Andaman earthquakes—imaging the boundary between the ruptures of the great 2004 and 2005 earthquakes. *Earth Planet. Sci. Lett.*, 269(1–2), 118–130.

Fruehn, J., von Huene, R., and Fisher, M. A. (1999). Accretion in the wake of terrane collision: The Neogene accretionary wedge off Kenai Peninsula, Alaska. *Tectonics*, 18(2), 263–277.

Funnell, M. J., Peirce, C., and Robinson, A. H. (2017). Structural variability of the Tonga-Kermadec forearc characterized using robustly constrained geophysical data. *Geophys. J. Int.*, 210(3), 1681–1702.

Gase, A. C., Bangs, N. L., Van Avendonk, H. J., Bassett, D., and Henrys, S. A. (2022). Hikurangi megathrust slip behavior influenced by lateral variability in sediment subduction. *Geology*, 50(10), 1145–1149.

Gase, A. C., Van Avendonk, H. J., Bangs, N. L., Bassett, D., Henrys, S. A., Barker, D. H. N., Kodaira, S., Jacobs, K. M., Luckie, T. W., Okaya, D. A., Fujie, G., Yamamoto, Y., Arnulf, A. F., and Arai, R. (2021). Crustal structure of the northern Hikurangi margin, New Zealand: Variable accretion and overthrusting plate strength influenced by rough subduction. *J. Geophys. Res.: Solid Earth*, 126(5), article no. e2020JB021176.

Gnibidenko, H., Bykova, T. G., Veselov, O. V., Vorobiev, V. M., and Svarichevsky, A. S. (1983). The Tectonics of the Kuril-Kamchatka deep-sea trench. In Hilde, T. W. C. and Uyeda, S., editors, *Geodynamics of the Western Pacific-Indonesian Region*, volume 11 of *Geodynamics Series*, pages 249–286. American Geophysical Union, Washington, DC.

Gomez, S. (2018). *Tectonostratigraphic evolution of the Barbados accretionary prism and surrounding sedimentary basin within the southeastern Caribbean-South America plate boundary zone*. Phd thesis, Houston University. 233 pp.

González, F. A., Bello-González, J. P., Contreras-Reyes, E., Tréhu, A. M., and Geersen, J. (2023). Shallow structure of the Northern Chilean marine forearc between 19°S–21°S using multichannel seismic reflection and refraction data. *J. South Am. Earth Sci.*, 123, article no. 104243.

Górszczyk, A., Operto, S., Schenini, L., and Yamada, Y. (2019). Crustal-scale depth imaging via joint full-waveform inversion of ocean-bottom seismometer data and pre-stack depth migration of multichannel seismic data: a case study from the eastern Nankai Trough. *Solid Earth*, 10(3), 765–784.

Granja-Bruña, J., Carbó-Gorosabel, A., Estrada, P. L., Muñoz-Martín, A., Ten Brink, U. S., Gomez Ballesteros, M., Druet, M., and Pazos, A. (2014). Morphostructure at the junction between the Beata ridge and the Greater Antilles island arc (offshore Hispaniola southern slope). *Tectonophysics*, 618, 138–163.

Granja-Bruña, J., Ten Brink, U. S., Carbó-Gorosabel, A., Muñoz-Martín, A., and Ballesteros, M. G. (2009). Morphotectonics of the central Muertos thrust belt and Muertos Trough (northeastern Caribbean). *Mar. Geol.*, 263(1-4), 7–33.

Grevemeyer, I., Diaz-Naveas, J. L., Ranero, C. R., Villinger, H. W., and Leg, O. D. P. (2003). Heat flow over the descending Nazca plate in central Chile, 32 S to 41 S: Observations from ODP Leg 202 and the occurrence of natural gas hydrates. *Earth Planet. Sci. Lett.*, 213(3–4), 285–298.

Hamada, Y., Hirose, T., Ijiri, A., Yamada, Y., Sanada, Y., Saito, S., Sakurai, N., Sugihara, T., Yokoyama, T., Saruhashi, T., Hoshino, T., Kamiya, N., Bowden, S., Cramm, M., Henkel, S., Homola, K., Imachi, H., Kanedo, M., Lagostina, L., Manners, H., McClelland, H.-L., Metcalfe, K., Okutsu, N., Pan, D., Raudsepp, M. J., Sauvage, J., Schubotz, F., Spivack, A., Tonai, S., Treude, T., Tsang, M.-Y., Viehweger, B., Wang, D. T., Whitaker, E., Yamamoto, Y., Yang, K., Kinoshita, M., Maeda, L., Kubo, Y., Morono, Y., Inagaki, Y. F., and Heuer, V. B. (2018). In-situ mechanical weakness of subducting sediments beneath a plate boundary décollement in the Nankai Trough. *Prog. Earth Planet. Sci.*, 5(1), 1–10.

Hampel, A., Kukowski, N., Bialas, J., Huebscher, C., and Heinbockel, R. (2004). Ridge subduction at an erosive margin: The collision zone of the Nazca Ridge in southern Peru. *J. Geophys. Res.: Solid Earth*, 109(B2), article no. B02101.

Han, S., Bangs, N. L., Carbotte, S. M., Saffer, D. M., and Gibson, J. C. (2017). Links between sediment consolidation and Cascadia megathrust slip behaviour. *Nat. Geosci.*, 10(12), 954–959.

Hayes, D. E. and Lewis, S. D. (1984). A geophysical study of the Manila Trench, Luzon, Philippines: 1. Crustal structure, gravity, and regional tectonic evolution. *J. Geophys. Res.: Solid Earth*, 89(B11), 9171–9195.

Heuret, A. (2005). *Dynamique des zones de subduction: étude statistique globale et approche analogique*. Doctoral dissertation, Université Montpellier II-Sciences et Techniques du Languedoc.

Hinz, K., von Huene, R., Ranero, C. R., and PACOMAR Working Group (1996). Tectonic structure of the convergent Pacific margin offshore Costa Rica from multichannel seismic reflection data. *Tectonics*, 15(1), 54–66.

Horine, R. L., Moore, G. F., and Taylor, B. (1990). Structure of the outer Izu-Bonin forearc from seismic-reflection profiling and gravity modeling. In *Proceedings of the Ocean Drilling Program*, volume 125 of *Initial Reports*, pages 81–94. Ocean Drilling Program, College Station, TX.

Hsu, H. H., Liu, C. S., Chen, T. T., and Hung, H. T. (2021). Stratigraphic framework and sediment wave fields associated with canyon-levee systems in the Huatung Basin offshore Taiwan Orogen. *Mar. Geol.*, 433, article no. 106408.

Hsu, S. K., Yeh, Y. C., Sibuet, J. C., Doo, W. B., and Tsai, C. H. (2013). A mega-splay fault system and tsunami hazard in the southern Ryukyu subduction zone. *Earth Planet. Sci. Lett.*, 362, 99–107.

Huguen, C., Mascle, J., Chaumillon, E., Woodside, J. M., Benkhelil, J., Kopf, A., and Volkonskaïa, A. (2001). Deformational styles of the eastern Mediterranean Ridge and surroundings from combined swath mapping and seismic reflection profiling. *Tectonophysics*, 343(1–2), 21–47.

Jicha, B. R. and Kay, S. M. (2018). Quantifying arc migration and the role of forearc subduction erosion in the central Aleutians. *J. Volcanol. Geotherm. Res.*, 360, 84–99.

Klaeschen, D., Belykh, I., Gnibidenko, H., Patrikeyev, S., and von Huene, R. (1994). Structure of the Kuril Trench from seismic reflection records. *J. Geophys. Res.: Solid Earth*, 99(B12), 24173–24188.

Kodaira, S., Iidaka, T., Kato, A., Park, J. O., Iwasaki, T., and Kaneda, Y. (2004). High pore fluid pressure may cause silent slip in the Nankai Trough. *Science*, 304(5675), 1295–1298.

Kodaira, S., Kurashimo, E., Park, J. O., Takahashi, N., Nakanishi, A., Miura, S., Iwasaki, T., Hirata, N., Ito, K., and Kaneda, Y. (2002). Structural factors controlling the rupture process of a megathrust earthquake at the Nankai trough seismogenic zone. *Geophys. J. Int.*, 149(3), 815–835.

Kodaira, S., No, T., Nakamura, Y., Fujiwara, T., Kaiho, Y., Miura, S., Takahashi, N., Kaneda, Y., and Taira, A. (2012). Coseismic fault rupture at the trench axis during the 2011 Tohoku-oki earthquake. *Nat. Geosci.*, 5(9), 646–650.

Kopp, C., Fruehn, J., Flueh, E. R., Reichert, C., Kukowski, N., Bialas, J., and Klaeschen, D. (2000). Structure of the Makran subduction zone from wide-angle and reflection seismic data. *Tectonophysics*, 329(1–4), 171–191.

Kopp, H. (2011). The Java convergent margin: structure, seismogenesis and subduction processes. *Geol. Soc., Lond. Spec. Publ.*, 355(1), 111–137.

Kopp, H., Hindle, D., Klaeschen, D., Oncken, O., Reichert, C., and Scholl, D. (2009). Anatomy of the western Java plate interface from depth-migrated seismic images. *Earth Planet. Sci. Lett.*, 288(3–4), 399–407.

Kroehler, M. E., Mann, P., Escalona, A., and Christeson, G. L. (2011). Late Cretaceous-Miocene diachronous onset of back thrusting along the South Caribbean deformed belt and its importance for understanding processes of arc collision and crustal growth. *Tectonics*, 30(6), article no. TC6003.

Ku, C. Y. and Hsu, S. K. (2009). Crustal structure and deformation at the northern Manila Trench between Taiwan and Luzon islands. *Tectonophysics*, 466(3–4), 229–240.

Ladd, J. W., Ibrahim, A. K., McMillen, K. J., Latham, G. V., and von Huene, R. (1982). Interpretation of seismic-reflection data of the Middle America Trench offshore Guatemala. *Initial Rep. Deep Sea Drill. Proj.*, 67, 675–689.

Ladd, J. W., Truchan, M., Talwani, M., Stoffa, P. L., Buhl, P., Houtz, R., Mauffret, A., and Westbrook, G. (1984). Seismic reflection profiles across the southern margin of the Caribbean. In *The Caribbean-South American Plate Boundary and Regional Tectonics*, Geological Society of America Memoir, 162, pages 153–160. Geological Society of America, Boulder, CO.

Laigle, M., Becel, A., de Voogd, B., Sachpazi, M., Bayrakci, G., Lebrun, J. F., and Evain, M. (2013). Along-arc segmentation and interaction of subducting ridges with the Lesser Antilles Subduction forearc crust revealed by MCS imaging. *Tectonophysics*, 603, 32–54.

Lallemand, S., Chamot-Rooke, N., and Aubouin, J. (1986). Sur la cause du décrochement senestre entre les fosses du Japon et des Kouriles: subduction-collision d'un ancien volcan sous-marin. *C. R. Acad. Sci., Paris, Sér. B*, 303(16), 1443–1448.

Lallemand, S., Theunissen, T., Schnürle, P., Lee, C.-S., Liu, C.-S., and Font, Y. (2013). Indentation of the Philippine Sea Plate by the Eurasia Plate in Taiwan: details from recent marine seismological experiments. *Tectonophysics*, 594, 60–79.

Lallemand, S. E., Popoff, M., Cadet, J. P., Bader, A. G., Pubellier, M., Rangin, C., and Deffontaines, B. (1998). Genetic relations between the central and southern Philippine Trench and the Sangihe Trench. *J. Geophys. Res.: Solid Earth*, 103(B1), 933–950.

Lallemant, S., Truffert, C., Jolivet, L., Henry, P., Chamot-Rooke, N., and De Voogd, B. (1994). Spatial transition from compression to extension in the Western Mediterranean Ridge accretionary complex. *Tectonophysics*, 234(1–2), 33–52.

Lamarche, G. and Lebrun, J. F. (2000). Transition from strike-slip faulting to oblique subduction: active tectonics at the Puysegur Margin, South New Zealand. *Tectonophysics*, 316(1–2), 67–89.

Larter, R. D., Vanneste, L. E., Morris, P., and Smythe, D. K. (2003). Structure and tectonic evolution of the South Sandwich arc. *Geol. Soc. Lond. Special Publications*, 219(1), 255–284.

Laurencin, M. (2017). *Etude de la géométrie, de la nature et des déformations de la zone de subduction des Petites Antilles du Nord*. Phd thesis, University of Bretagne Loire, Brest. 294 pp.

Lebrun, J. F., Lamarche, G., Collot, J. Y., and Delteil, J. (2000). Abrupt strike-slip fault to subduction transition: The Alpine fault-Puysegur trench connection, New Zealand. *Tectonics*, 19(4), 688–706.

Lester, R., McIntosh, K., Van Avendonk, H. J., Lavier, L., Liu, C. S., and Wang, T. K. (2013). Crustal accretion in the Manila trench accretionary wedge at the transition from subduction to mountain-building in Taiwan. *Earth Planet. Sci. Lett.*, 375, 430–440.

Lewis, K. B., Collot, J. Y., and Lallemand, S. E. (1998). The dammed Hikurangi Trough: a channel-fed trench blocked by subducting seamounts and their wake avalanches (New Zealand–France GeodyNZ Project). *Basin Res.*, 10(4), 441–468.

Lewis, S. D., Ladd, J. W., and Bruns, T. R. (1988). Structural development of an accretionary prism by thrust and strike-slip faulting: Shumagin region, Aleutian Trench. *Geol. Soc. Am. Bull.*, 100(5), 767–782.

Ma, B., Geersen, J., Klaeschen, D., Contreras-Reyes, E., Riedel, M., Xia, Y., Tréhu, A. M., Lange, D., and

Kopp, H. (2023). Impact of the Iquique Ridge on structure and deformation of the north Chilean subduction zone. *J. South Am. Earth Sci.*, 124, article no. 104262.

Ma, B., Geersen, J., Lange, D., Klaeschen, D., Grevemeyer, I., Contreras-Reyes, E., Petersen, F., Riedel, M., Xia, Y., Tréhu, A. M., and Kopp, H. (2022). Megathrust reflectivity reveals the updip limit of the 2014 Iquique earthquake rupture. *Nat. Commun.*, 13(1), article no. 3969.

MacKay, M. E. and Moore, G. F. (1990). Variation in deformation of the south Panama accretionary prism: Response to oblique subduction and trench sediment variation. *Tectonics*, 9(4), 683–698.

Maesano, F. E., Tiberti, M. M., and Basili, R. (2017). The Calabrian Arc: three-dimensional modelling of the subduction interface. *Sci. Rep.*, 7(1), 1–15.

Mantilla-Pimiento, A. M., Jentzsch, G., Kley, J., and Alfonso-Pava, C. (2009). Configuration of the Colombian Caribbean Margin: Constraints from 2D seismic reflection data and potential fields interpretation. In Lallemand, S. and Funiciello, F., editors, *Subduction Zone Geodynamics*, pages 247–272. Springer, Berlin.

Marcaillou, B., Collot, J. Y., Ribodetti, A., d'Acremont, E., Mahamat, A. A., and Alvarado, A. (2016). Seamount subduction at the North-Ecuadorian convergent margin: Effects on structures, interseismic coupling and seismogenesis. *Earth Planet. Sci. Lett.*, 433, 146–158.

Marcaillou, B., Klingelhoefer, F., Laurencin, M., Lebrun, J. F., Laigle, M., Lallemand, S., Schenini, L., Gay, A., Boucard, M., Ezenkawa, K., and Graindorge, D. (2021). Pervasive detachment faults within the slow spreading oceanic crust at the poorly coupled Antilles subduction zone. *Commun. Earth Environ.*, 2(1), article no. 203.

Marcaillou, B., Spence, G., Collot, J. Y., and Wang, K. (2006). Thermal regime from bottom simulating reflectors along the north Ecuador–south Colombia margin: Relation to margin segmentation and great subduction earthquakes. *J. Geophys. Res.: Solid Earth*, 111(B12), article no. B12407.

Mazzotti, S., Lallemant, S. J., Henry, P., Le Pichon, X., Tokuyama, H., and Takahashi, N. (2002). Intraplate shortening and underthrusting of a large basement ridge in the eastern Nankai subduction zone. *Mar. Geol.*, 187(1–2), 63–88.

McCarthy, J. and Scholl, D. W. (1985). Mechanisms of subduction accretion along the central Aleutian Trench. *Geol. Soc. Am. Bull.*, 96(6), 691–701.

McIntosh, K., van Avendonk, H., Lavier, L., Lester, W. R., Eakin, D., Wu, F., Liu, C.-S., and Lee, C. S. (2013). Inversion of a hyper-extended rifted margin in the southern Central Range of Taiwan. *Geology*, 41(8), 871–874.

McNeill, L. C. and Henstock, T. J. (2014). Forearc structure and morphology along the Sumatra-Andaman subduction zone. *Tectonics*, 33(2), 112–134.

Milsom, J., Kaye, S., and Sardjono, S. (1996). Extension, collision and curvature in the eastern Banda arc. *Geol. Soc., Lond., Spec. Publ.*, 106(1), 85–94.

Moeremans, R., Singh, S. C., Mukti, M., McArdle, J., and Johansen, K. (2014). Seismic images of structural variations along the deformation front of the Andaman–Sumatra subduction zone: implications for rupture propagation and tsunamigenesis. *Earth Planet. Sci. Lett.*, 386, 75–85.

Moore, G. F. and Shipley, T. H. (1988). Mechanisms of sediment accretion in the Middle America Trench off Mexico. *J. Geophys. Res.: Solid Earth*, 93(B8), 8911–8927.

Moore, G. F., Shipley, T. H., and Lonsdale, P. F. (1986). Subduction erosion versus sediment offscraping at the toe of the Middle America Trench off Guatemala. *Tectonics*, 5(4), 513–523.

Moore, G. F., Shipley, T. H., Stoffa, P. L., Karig, D. E., Taira, A., Kuramoto, S., Tokuyama, H., and Suyehiro, K. (1990). Structure of the Nankai Trough accretionary zone from multichannel seismic reflection data. *J. Geophys. Res.: Solid Earth*, 95(B6), 8753–8765.

Morena, P., Ratzov, G., Cattaneo, A., Klingelhoefer, F., Beck, C., Seibert, C., Marcaillou, B., and Feuillet, N. (2022). Coexistence of adjacent siliciclastic, carbonate, and mixed sedimentary systems: An example from seafloor morphology in the Northern Lesser Antilles Forearc. *Front. Earth Sci.*, 10, article no. 834029.

Myers, E. K., Roland, E. C., Tréhu, A. M., Davenport, K., and PICTURES group (2022). Crustal structure of the incoming iquique ridge offshore Northern Chile. *J. Geophys. Res.: Solid Earth*, 127(2), article no. e2021JB023169.

Nikolinakou, M. A., Flemings, P. B., Gao, B., and Saffer, D. M. (2023). The evolution of pore pressure, stress, and physical properties during sediment accretion at subduction zones. *J. Geophys. Res.: Solid Earth*, 128, article no. e2022JB025504.

Nishizawa, A., Kaneda, K., and Oikawa, M. (2009). Seismic structure of the northern end of the Ryukyu Trench subduction zone, southeast of Kyushu, Japan. *Earth Planet. Space*, 61, e37–e40.

Nishizawa, A., Kaneda, K., Oikawa, M., Horiuchi, D., Fujioka, Y., and Okada, C. (2017). Variations in seismic velocity distribution along the Ryukyu (Nansei-Shoto) Trench subduction zone at the northwestern end of the Philippine Sea plate. *Earth Planet. Space*, 69, 1–17.

Oakley, A. J., Taylor, B., and Moore, G. F. (2008). Pacific Plate subduction beneath the central Mariana and Izu-Bonin fore arcs: New insights from an old margin. *Geochem. Geophys. Geosyst.*, 9(6), article no. Q06003.

Okamura, Y., Nishizawa, A., Oikawa, M., and Horiuchi, D. (2017). Differential subsidence of the forearc wedge of the Ryukyu (Nansei-Shoto) Arc caused by subduction of ridges on the Philippine Sea Plate. *Tectonophysics*, 717, 399–412.

Pairault, A. A., Hall, R., and Elders, C. F. (2003). Structural styles and tectonic evolution of the Seram Trough, Indonesia. *Mar. Petrol. Geol.*, 20(10), 1141–1160.

Pajang, S., Khatib, M. M., Heyhat, M., Cubas, N., Bessiere, E., Letouzey, J., Mokhtari, M., and Le Pourhiet, L. (2022). The distinct morphologic signature of underplating and seamounts in accretionary prisms, insights from thermomechanical modeling applied to Coastal Iranian Makran. *Tectonophysics*, 845, article no. 229617.

Park, J. O., Hori, T., and Kaneda, Y. (2009). Seismotectonic implications of the Kyushu-Palau ridge subducting beneath the westernmost Nankai forearc. *Earth, Planet. Space*, 61, 1013–1018.

Park, J. O. and Kodaira, S. (2012). Seismic reflection and bathymetric evidences for the Nankai earthquake rupture across a stable segment-boundary. *Earth Planet. Space*, 64(3), 299–303.

Park, J. O., Naruse, H., and Bangs, N. L. (2014). Along-strike variations in the Nankai shallow décollement properties and their implications for tsunami earthquake generation. *Geophys. Res. Lett.*, 41(20), 7057–7064.

Park, J. O., Tokuyama, H., Shinohara, M., Suyehiro, K., and Taira, A. (1998). Seismic record of tectonic evolution and backarc rifting in the southern Ryukyu island arc system. *Tectonophysics*, 294(1–2), 21–42.

Park, J. O., Tsuru, T., Kodaira, S., Nakanishi, A., Miura, S., Kaneda, Y., Kono, Y., and Takahashi, N. (2000). Out-of-sequence thrust faults developed in the coseismic slip zone of the 1946 Nankai earthquake (Mw = 8.2) off Shikoku, southwest Japan. *Geophys. Res. Lett.*, 27(7), 1033–1036.

Park, J. O., Tsuru, T., Takahashi, N., Hori, T., Kodaira, S., Nakanishi, A., Miura, S., and Kaneda, Y. (2002). A deep strong reflector in the Nankai accretionary wedge from multichannel seismic data: Implications for underplating and interseismic shear stress release. *J. Geophys. Res.: Solid Earth*, 107(B4), article no. ESE-3.

Parvaiz, S., Ali, A., Javed, F., and Shah, M. A. (2022). Deformational pattern and seismogenic potential of the eastern Makran subduction zone. *J. Asian Earth Sci.*, 235, article no. 105298.

Pecher, I. A., Kukowski, N., Huebscher, C., Greinert, J., Bialas, J., and GEOPECO Working Group (2001). The link between bottom-simulating reflections and methane flux into the gas hydrate stability zone–new evidence from Lima Basin, Peru Margin. *Earth Planet. Sci. Lett.*, 185(3–4), 343–354.

Petersen, F., Lange, D., Ma, B., Grevemeyer, I., Geersen, J., Klaeschen, D., Contreras-Reyes, E., Barrientos, S., Tréhu, A. M., Vera, E., and Kopp, H. (2021). Relationship between subduction erosion and the up-dip limit of the 2014 Mw 8.1 Iquique earthquake. *Geophys. Res. Lett.*, 48(9), article no. e2020GL092207.

Pichot, T., Patriat, M., Westbrook, G. K., Nalpas, T., Gutscher, M. A., Roest, W. R., Deville, E., Moulin, M., Aslanian, D., and Rabineau, M. (2012). The Cenozoic tectonostratigraphic evolution of the Barracuda Ridge and Tiburon Rise, at the western end of the North America–South America plate boundary zone. *Mar. Geol.*, 303, 154–171.

Polonia, A., Torelli, L., Brancolini, G., and Loreto, M. F. (2007). Tectonic accretion versus erosion along the southern Chile trench: Oblique subduction and margin segmentation. *Tectonics*, 26(3), article no. TC3005.

Polonia, A., Torelli, L., Gasperini, L., Cocchi, L., Muccini, F., Bonatti, E., Hensen, C., Schmidt, M., Romano, S., Artoni, A., and Carlini, M. (2017). Lower plate serpentinite diapirism in the Calabrian Arc subduction complex. *Nat. Commun.*, 8(1), article no. 2172.

Prada, M., Bartolomé, R., Gras, C., Bandy, W. L., and Dañobeitia, J. J. (2023). Trench-parallel ridge subduction controls upper-plate structure and shallow megathrust seismogenesis along the Jalisco-Colima margin, Mexico. *Commun. Earth Environ.*, 4(1), article no. 53.

Ranero, C. R., Grevemeyer, I., Sahling, H., Barckhausen, U., Hensen, C., Wallmann, K., Weinrebe, W., Vannucchi, P., von Huene, R., and McIntosh, K. (2008). Hydrogeological system of erosional convergent margins and its influence on tectonics and interplate seismogenesis. *Geochem. Geophys. Geosyst.*, 9(3), article no. Q03S04.

Ranero, C. R., Phipps Morgan, J., McIntosh, K., and Reichert, C. (2003). Bending-related faulting and mantle serpentinization at the Middle America trench. *Nature*, 425(6956), 367–373.

Ranero, C. R. and von Huene, R. (2000). Subduction erosion along the Middle America convergent margin. *Nature*, 404(6779), 748–752.

Ranero, C. R., Von Huene, R., Weinrebe, W., and Barckhausen, U. (2007). Convergent margin tectonics: a marine perspective. In *Central America, Geology, Resources, Hazards*, volume 1, pages 239–265. Taylor & Francis, London.

Rodríguez-Zurrunero, A., Granja-Bruña, J. L., Carbó-Gorosabel, A., Muñoz-Martín, A., Gorosabel-Araus, J. M., Gómez de la Peñac, L., Gómez Ballesteros, M., Pazos, A., Catalán, M., Espinosa, S., Druet, M., Llanes, P., and ten Brink, U. (2020a). Submarine morpho-structure and active processes along the North American-Caribbean plate boundary (Dominican Republic sector). *Mar. Geol.*, 407, 121–147.

Rodríguez-Zurrunero, A., Granja-Bruña, J. L., Muñoz-Martín, A., Leroy, S., ten Brink, U., Gorosabel-Araus, J. M., Gómez de la Peña, L., Druet, M., and Carbó-Gorosabel, A. (2020b). Along-strike segmentation in the northern Caribbean plate boundary zone (Hispaniola sector): Tectonic implications. *Tectonophysics*, 776, article no. 228322.

Ryan, H. F. and Scholl, D. W. (1989). The evolution of forearc structures along an oblique convergent margin, central Aleutian arc. *Tectonics*, 8(3), 497–516.

Sage, F., Collot, J. Y., and Ranero, C. R. (2006). Interplate patchiness and subduction-erosion mechanisms: Evidence from depth-migrated seismic images at the central Ecuador convergent margin. *Geology*, 34(12), 997–1000.

Sanchez, J., Mann, P., Carvajal-Arenas, L. C., and Bernal-Olaya, R. (2019). Regional transect across the western Caribbean Sea based on integration of geologic, seismic reflection, gravity, and magnetic data. *AAPG Bull.*, 103(2), 303–343.

Scherwath, M., Contreras-Reyes, E., Flueh, E. R., Grevemeyer, I., Krabbenhöft, A., Papenberg, C., Petersen, C. J., and Weinrebe, R. W. (2009). Deep lithospheric structures along the southern central Chile margin from wide-angle P-wave modelling. *Geophys. J. Int.*, 179(1), 579–600.

Scherwath, M., Kopp, H., Flueh, E. R., Henrys, S. A., Sutherland, R., Stagpoole, V. M., Barker, D. H. N., Reyners, M. E., Bassett, D. G., Planert, L., and Dannowski, A. (2010). Fore-arc deformation and underplating at the northern Hikurangi margin, New Zealand. *J. Geophys. Res.: Solid Earth*, 115(B6), article no. B06408.

Schnürle, P., Lallemand, S. E., von Huene, R., and Klaeschen, D. (1995). Tectonic regime of the southern Kurile Trench as revealed by multichannel seismic lines. *Tectonophysics*, 241(3–4), 259–277.

Schnürle, P., Liu, C. S., Lallemand, S. E., and Reed, D. L. (1998). Structural insight into the south Ryukyu margin: Effects of the subducting Gagua Ridge. *Tectonophysics*, 288(1-4), 237–250.

Scholl, D. W., Kirby, S. H., von Huene, R., Ryan, H., Wells, R. E., and Geist, E. L. (2015). Great (≥ Mw8.0) megathrust earthquakes and the subduction of excess sediment and bathymetrically smooth seafloor. *Geosphere*, 11(2), 236–265.

Scholl, D. W., Vallier, T. L., and Stevenson, A. J. (1982). Sedimentation and deformation in the Amlia fracture zone sector of the Aleutian trench. *Mar. Geol.*, 48(1–2), 105–134.

Shipley, T. H., McIntosh, K. D., Silver, E. A., and Stoffa, P. L. (1992). Three-dimensional seismic imaging of the Costa Rica accretionary prism: Structural diversity in a small volume of the lower slope. *J. Geophys. Res.: Solid Earth*, 97(B4), 4439–4459.

Shipley, T. H. and Moore, G. F. (1985). Sediment accretion and subduction in the Middle America Trench. In Nasu, N. et al., editors, *Advances in Earth and Planetary Sciences. Formation of Active Ocean Margins*, pages 221–256. Terra Scientific, Tokyo.

Shipley, T. H. and Moore, G. F. (1986). Sediment accretion, subduction, and dewatering at the base of the trench slope off Costa Rica: A seismic reflection view of the décollement. *J. Geophys. Res.: Solid*

Earth, 91(B2), 2019–2028.

Shipley, T. H., Stoffa, P. L., and Dean, D. F. (1990). Underthrust sediments, fluid migration paths, and mud volcanoes associated with the accretionary wedge off Costa Rica: Middle America Trench. *J. Geophys. Res.: Solid Earth*, 95(B6), 8743–8752.

Shulgin, A., Kopp, H., Mueller, C., Planert, L., Lueschen, E., Flueh, E. R., and Djajadihardja, Y. (2011). Structural architecture of oceanic plateau subduction offshore Eastern Java and the potential implications for geohazards. *Geophys. J. Int.*, 184(1), 12–28.

Silver, E. A., Reed, D., McCaffrey, R., and Joyodiwiryo, Y. (1983). Back arc thrusting in the eastern Sunda arc, Indonesia: A consequence of arc-continent collision. *J. Geophys. Res.: Solid Earth*, 88(B9), 7429–7448.

Silver, E. A., Reed, D. L., Tagudin, J. E., and Heil, D. J. (1990). Implications of the north and south Panama thrust belts for the origin of the Panama orocline. *Tectonics*, 9(2), 261–281.

Speed, R. C. and Larue, D. K. (1982). Barbados: Architecture and implications for accretion. *J. Geophys. Res.: Solid Earth*, 87(B5), 3633–3643.

Stratford, W., Peirce, C., Paulatto, M., Funnell, M., Watts, A. B., Grevemeyer, I., and Bassett, D. (2015). Seismic velocity structure and deformation due to the collision of the Louisville Ridge with the Tonga-Kermadec Trench. *Geophys. J. Int.*, 200(3), 1503–1522.

Takahashi, N., Amano, H., Hirata, K., Kinoshita, H., Lallemant, S., Tokuyama, H., Yamamoto, F., Taira, A., and Suyehiro, K. (2002a). Faults configuration around the eastern Nankai trough deduced by multichannel seismic profiling. *Mar. Geol.*, 187(1–2), 31–46.

Takahashi, N., Kodaira, S., Nakanishi, A., Park, J. O., Miura, S., Tsuru, T., Kaneda, Y., Suyehiro, K., Kinoshita, H., Hirata, N., and Iwasaki, T. (2002b). Seismic structure of western end of the Nankai trough seismogenic zone. *J. Geophys. Res.: Solid Earth*, 107(B10), article no. ESE-2.

Takahashi, N., Suyehiro, K., and Shinohara, M. (1998). Implications from the seismic crustal structure of the northern Izu–Bonin arc. *Isl. Arc*, 7(3), 383–394.

Ten Brink, U. (2005). Vertical motions of the Puerto Rico Trench and Puerto Rico and their cause. *J. Geophys. Res.: Solid Earth*, 110, article no. B06404.

Tobin, H., Vannucchi, P., and Meschede, M. (2001). Structure, inferred mechanical properties, and implications for fluid transport in the décollement zone, Costa Rica convergent margin. *Geology*, 29(10), 907–910.

Tobin, H. J., Moore, J. C., Mackay, M. E., Orange, D. L., and Kulm, L. D. (1993). Fluid flow along a strike-slip fault at the toe of the Oregon accretionary prism: Implications for the geometry of frontal accretion. *Geol. Soc. Am. Bull.*, 105(5), 569–582.

Tsuru, T., Park, J.-O., Miura, S., Kodaira, S., Kido, Y., and Hayashi, T. (2002). Along-arc structural variation of the plate boundary at the Japan Trench margin: Implication of interplate coupling. *J. Geophys. Res.*, 107(B12), 2357.

Tsuru, T., Park, J. O., Takahashi, N., Kodaira, S., Kido, Y., Kaneda, Y., and Kono, Y. (2000). Tectonic features of the Japan Trench convergent margin off Sanriku, northeastern Japan, revealed by multichannel seismic reflection data. *J. Geophys. Res.: Solid Earth*, 105(B7), 16403–16413.

Vanneste, L. E. and Larter, R. D. (2002). Sediment subduction, subduction erosion, and strain regime in the northern South Sandwich forearc. *J. Geophys. Res.: Solid Earth*, 107(B7), article no. EPM-5.

Vidal, N., Alvarez-Marrón, J., and Klaeschen, D. (2000). The structure of the Africa-Anatolia plate boundary in the eastern Mediterranean. *Tectonics*, 19(4), 723–739.

Von Huene, R. (1972). Structure of the continental margin and tectonism at the eastern Aleutian Trench. *Geol. Soc. Am. Bull.*, 83(12), 3613–3626.

von Huene, R., Bourgois, J., Miller, J., and Pautot, G. (1989). A large tsunamogenic landslide and debris flow along the Peru Trench. *J. Geophys. Res.: Solid Earth*, 94(B2), 1703–1714.

Von Huene, R., Corvalán, J., Flueh, E. R., Hinz, K., Korstgard, J., Ranero, C. R., and Weinrebe, W. (1997a). Tectonic control of the subducting Juan Fernández Ridge on the Andean margin near Valparaiso, Chile. *Tectonics*, 16(3), 474–488.

Von Huene, R. and Klaeschen, D. (1999). Opposing gradients of permanent strain in the aseismic zone and elastic strain across the seismogenic zone of the Kodiak shelf and slope, Alaska. *Tectonics*, 18(2), 248–262.

Von Huene, R., Klaeschen, D., Cropp, B., and Miller, J. (1994). Tectonic structure across the accretionary and erosional parts of the Japan Trench margin. *J.*

Geophys. Res.: Solid Earth, 99(B11), 22349–22361.

Von Huene, R., Kulm, L. D., and Miller, J. (1985). Structure of the frontal part of the Andean convergent margin. *J. Geophys. Res.: Solid Earth*, 90(B7), 5429–5442.

Von Huene, R. and Miller, J. (1986). *Seismic Images of Modern Convergent Margin Tectonic Structure*, volume 26 of *American Association of Petroleum Geologists Studies in Geology*. Tulsa, Oklahoma, USA.

von Huene, R., Miller, J. J., and Krabbenhoeft, A. (2021). The Alaska convergent margin backstop splay fault zone, a potential large tsunami generator between the frontal prism and continental framework. *Geochem. Geophys. Geosyst.*, 22(1), article no. e2019GC008901.

von Huene, R., Pecher, I. A., and Gutscher, M. A. (1996). Development of the accretionary prism along Peru and material flux after subduction of Nazca Ridge. *Tectonics*, 15(1), 19–33.

von Huene, R. and Ranero, C. R. (2003). Subduction erosion and basal friction along the sediment-starved convergent margin off Antofagasta, Chile. *J. Geophys. Res.: Solid Earth*, 108(B2), article no. 2079.

von Huene, R., Ranero, C. R., and Watts, P. (2004). Tsunamigenic slope failure along the Middle America Trench in two tectonic settings. *Mar. Geol.*, 203(3–4), 303–317.

von Huene, R., Ranero, C. R., Weinrebe, W., and Hinz, K. (2000). Quaternary convergent margin tectonics of Costa Rica, segmentation of the Cocos Plate, and Central American volcanism. *Tectonics*, 19(2), 314–334.

Von Huene, R., Reston, T., Kukowski, N., Dehghani, G. A., Weinrebe, W., and IMERSE Working Group (1997b). A subducting seamount beneath the Mediterranean Ridge. *Tectonophysics*, 271(3–4), 249–261.

Von Huene, R. and Scholl, D. (1991). Observations at convergent margins concerning sediment subduction, subduction erosion, and the growth of continental crust. *Rev. Geophys.*, 29(3), 279–316.

Wang, C. Y., Hwang, W. T., and Cochrane, G. R. (1994). Tectonic dewatering and mechanics of protothrust zones: example from the Cascadia accretionary margin. *J. Geophys. Res.: Solid Earth*, 99(B10), 20043–20050.

Wang, C. Y., Shi, Y., Hwang, W. T., and Chen, H. (1990). Hydrogeologic processes in the Oregon-Washington accretionary complex. *J. Geophys. Res.: Solid Earth*, 95(B6), 9009–9023.

Westbrook, G. K., Hardy, N. C., and Heath, R. P. (1995). Structure and tectonics of the Panama-Nazca plate boundary. In Mann, P., editor, *Geologic and Tectonic Development of the Caribbean Plate Boundary in Southern Central America*, Geological Society of America Special Paper, 295, pages 91–112. Geological Society of America, Boulder, CO.

Westbrook, G. K., Ladd, J. W., Buhl, P., Bangs, N., and Tiley, G. J. (1988). Cross section of an accretionary wedge: Barbados Ridge complex. *Geology*, 16(7), 631–635.

Wright, D. J., Bloomer, S. H., MacLeod, C. J., Taylor, B., and Goodlife, A. M. (2000). Bathymetry of the Tonga Trench and Forearc: a map series. *Mar. Geophys. Res.*, 21, 489–512.

Yang, Y., Wu, S., Gao, J., Tian, L., Yang, J., and Xu, Y. (2018). Geology of the Yap Trench: new observations from a transect near 10 N from manned submersible Jiaolong. *Int. Geol. Rev.*, 60(16), 1941–1953.

Yuan, T., Spence, G. D., and Hyndman, R. D. (1994). Seismic velocities and inferred porosities in the accretionary wedge sediments at the Cascadia margin. *J. Geophys. Res.: Solid Earth*, 99(B3), 4413–4427.

Zhang, Z., Dong, D., Sun, W., and Zhang, G. (2021). The Caroline Ridge fault system and implications for the bending-related faulting of incoming oceanic plateaus. *Gondwana Res.*, 92, 133–148.

Zhang, Z. Y., Dong, D. D., Sun, W. D., Wu, S. G., Bai, Y. L., Wang, X. J., and Fan, J. K. (2019). Subduction Erosion, crustal structure, and an evolutionary model of the northern yap subduction zone: New observations from the latest geophysical survey. *Geochem. Geophys. Geosyst.*, 20(1), 166–182.